Accepted Manuscript

Novel 4-(2-(benzo[d]thiazol-2-yl)phenoxy) substituted phthalocyanine derivatives: Synthesis, electrochemical and *in situ* spectroelectrochemical characterization

Asiye Nas, Halit Kantekin, Atıf Koca

PII: S0022-328X(14)00027-8

DOI: 10.1016/j.jorganchem.2014.01.012

Reference: JOM 18453

To appear in: *Journal of Organometallic Chemistry*

Received Date: 25 July 2013

Revised Date: 10 January 2014

Accepted Date: 13 January 2014

Please cite this article as: A. Nas, H. Kantekin, A. Koca, Novel 4-(2-(benzo[d]thiazol-2-yl)phenoxy) substituted phthalocyanine derivatives: Synthesis, electrochemical and *in situ* spectroelectrochemical characterization, *Journal of Organometallic Chemistry* (2014), doi: 10.1016/j.jorganchem.2014.01.012.

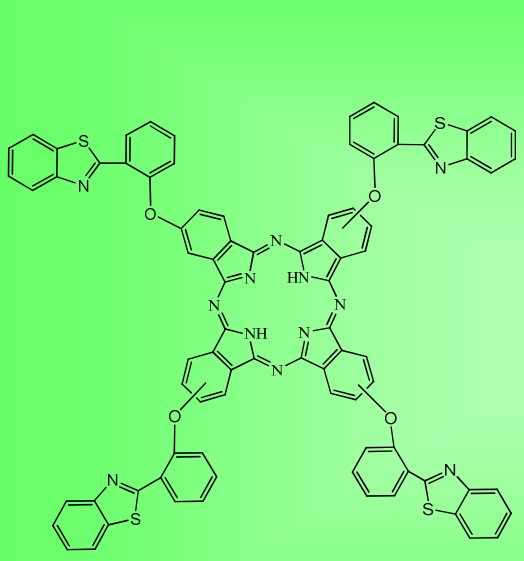

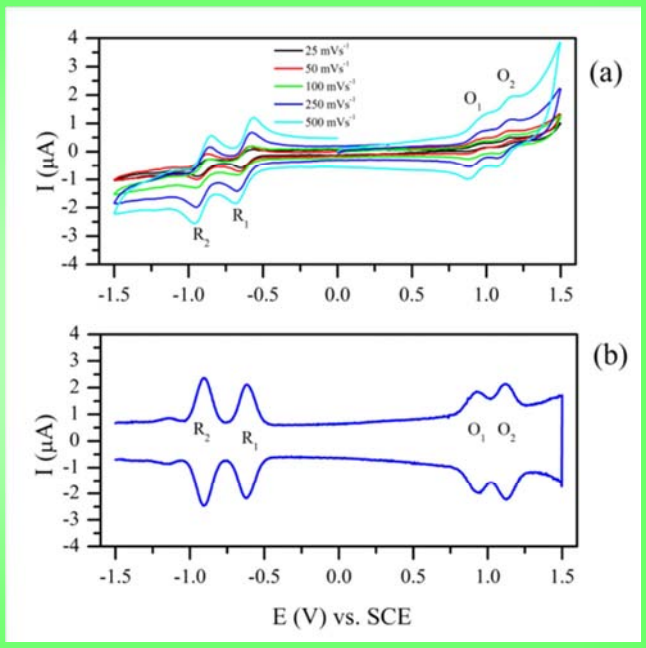

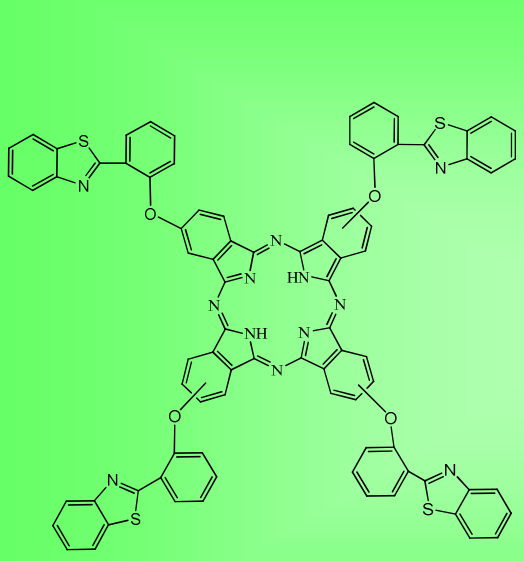

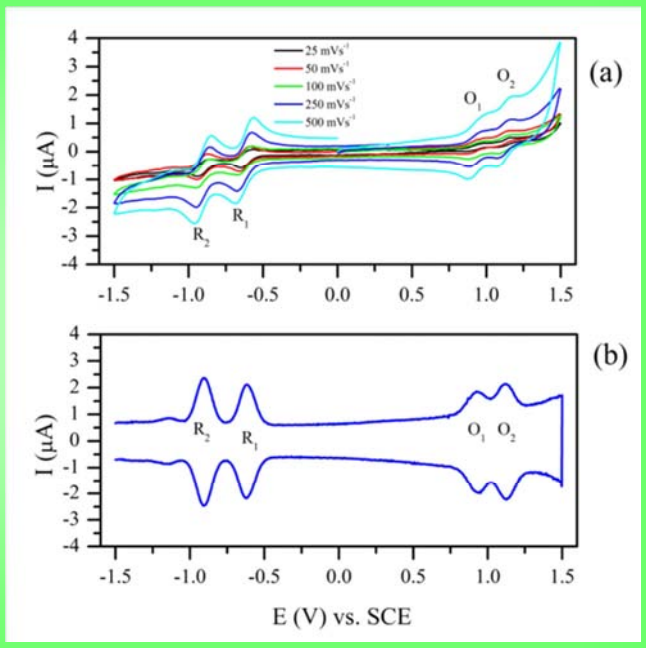

Novel 4-(2-(benzo[d]thiazol-2-yl)phenoxy) substituted phthalocyanine derivatives: Synthesis, electrochemical and *in situ* spectroelectrochemical characterization

Asiye Nas[a], Halit Kantekin[a*], Atıf Koca[b]

[a]*Department of Chemistry, Karadeniz Technical University, 61080, Trabzon-Turkey*

[b]*Department of Chemical Engineering, Engineering Faculty, Marmara University, 34722 Göztepe, İstanbul-Turkey*

*Corresponding author. Tel.: +90 462 377 25 89 fax: +90 462 325 31 96
E-mail address: halit@ktu.edu.tr (H. Kantekin)

Abstract

In this study, the new tetra peripherally 4-(2-(benzo[d]thiazol-2-yl)phenoxy)-substituted metal-free (**4**), zinc(II) (**5**), lead(II) (**6**), cobalt(II) (**7**) and copper(II) (**8**) phthalocyanine derivatives, which are organo-soluble, have been synthesized for the first time and their structures characterized by using electronic absorption, infrared spectroscopy, nuclear magnetic resonance spectroscopy, elemental analysis and mass spectra. Voltammetric characterization of the phthalocyanine derivatives (**4-7**) was performed with cyclic voltammetry and square wave voltammetry. Cobalt phthalocyanine (**7**) gave metal based electron transfer reactions in addition to the phthalocyanine ring based reduction and oxidation reactions. Although lead phthalocyanine (**6**) illustrated reversible reduction process during the voltammetric measurements, it was de-metallized and thus it turned back to the metal free phthalocyanine during the *in situ* spectroelectrochemical measurements under the applied potentials. Spectroelectrochemical measurements were performed to assign the redox processes and spectroscopic responses of the electrogenerated species.

Keywords: Benzothiazole; Metallophthalocyanine; Metal-free phthalocyanine; Electrochemistry; Demetallation.

1. Introduction

Metal complexes of N_4-ligands, such as porphyrins and phthalocyanines, are widely studied due to their numerous physical-chemical properties and the great variety of their applications in many fields [1]. Both series of phthalocyanines and porphyrins (tetrapyrrole macrocyles) are able to form several complexes with almost all the metals in Periodic Table [2] and it is known that at least seventy metal phthalocyanines have been prepared [3] thanks to their ability. Their favorable properties, such as extraordinary thermal and chemical stability, make them suitable as industrial pigments for a couple of decades [4].

Phthalocyanines, which are an important class of compounds use in inks, dyestuff for textiles and colorant for metals and plastics [5], have been used other applications such as liquid crystal displays [6, 7], optical applications [8, 9], electrochromism [10, 11], chemical sensors [12, 13], semiconductors for organic field-effect transistors (OFETs) [2, 14] and photodynamic therapy [15-17].

Photodynamic therapy (PDT) is a new technique that uses a photosensitizing agent and a particular type of light [18]. Metallophthalocyanines which can be used as photosensitizing agent for photodynamic therapy have received increasing attention since 1985 [19]. This therapy results in a sequence of photochemical and photobiological processes that cause irreversible photo damage to tumor tissues [20].

For all applications mentioned, the solubility of phthalocyanine derivatives plays a consequential role. Metallophthalocyanines are unsoluble in aqueous solvent in the absence of hydrophilic peripheral substituents but dissolve in strongly coordinating solvents like pyridine [21]. The bulky peripheral substitution on phthalocyanine core is used for enhancing the solubility of phthalocyanine derivatives in most common organic solvents; whereas sulfo or quaternary ammonium groups enhance solubility in aqueous media [22].

Thiazoles, which are a class of organic compounds, contain three carbon atoms, one nitrogen atom, and one sulfur atom. Among the pentaatomic heterocyclic rings, thiazole is one of the most intensively investigated. Thiazoles and their derivatives exhibit a wide variety of biological activities [23]. The number of annual publications dealing with thiazoles is continuously growing, but there are very few articles about thiazole substituted phthalocyanines in literature [24-26]. Because of this reason, in this work, the thiazole substituted metal-free (H_2Pc) and metallophthalocyanines (MPcs) were synthesized.

MPcs are used in many electrochemical technologies, especially electrosensing [27-30], electrochromic [31-33], and electrocatalytic [34-37] application due to the excellent redox properties. Changing the central metal and types, number and position of substituents alter molecule's the electrochemical responses as well as the usage fields of the MPc complexes [38-40].

Here, we report the synthesis and characterization of novel *4-(2-(benzo[d]thiazol-2-yl)phenoxy*-substituted **H_2Pc** (**4**), **ZnPc** (**5**), **PbPc** (**6**), **CoPc** (**7**) and **CuPc** (**8**) compounds. In this paper we aimed to investigate the electrochemical properties and possible application fields of the newly synthesized MPc complexes. Voltammetric characterizations of the phthalocyanines (**4-7**) were performed with cyclic voltammetry and square wave voltammetry for the first time. These organo-soluble phthalocyanines (**4-8**) have also been characterized by using electronic absorption, FT-IR, ^{1}H NMR, ^{13}C NMR, elemental analysis and mass spectra.

2. Experimental

2.1. Materials

All reagents and solvents were dried and purified as described in Perrin and Armarego [40]. 2-(benzo[d]thiazol-2-yl)phenol (**1**) was obtained from commercial supplier. *4*-nitro phthalonitrile (**2**) [41] was prepared according to the reported procedure. All other reagents and solvents were reagent grade quality and were obtained from commercial suppliers.

2.2. Equipments

Infrared spectra were recorded on a Perkin-Elmer FT-IR spectrometer Frontier. Elemental analyses were obtained from Costech ECS 4010 Spectrometer Elemental Analyzer (C, H, N). ^{1}H NMR and ^{13}C NMR spectra were recorded in $CDCl_3$ solvent on a Varian Mercury 200 MHz spectrometer (at Karadeniz Technical University, Turkey) and Varian Mercury 300 MHz spectrometer (at Sakarya University, Turkey) using TMS as an internal reference. Mass spectra were performed on a Brucker Microflex LT MALDI-TOF MS spectrometer (at Gebze Institute of Technology, Turkey). Optical spectra in the UV/Vis region were recorded with a Perkin Elmer Lambda 25 UV-Vis Spectrometer operating in the range 200-800 nm with quartz cells at the room temperature. Melting points were measured on an electrothermal melting point apparatus and were uncorrected.

All electrochemical measurements were carried out with Gamry Reference 600 potentiostat/galvanostat (at Marmara University, Turkey). An electrochemical cell with a three-electrode configuration was utilized with a Pt disc working electrode (surface area: 0.071 cm^2), a Pt wire counter electrode and saturated calomel reference electrode (SCE).

Electrochemical grade TBAP in extra pure DCM was employed as the supporting electrolyte at a concentration of 0.10 mol dm^{-3}.

An Ocean Optics QE65000 diode array spectrophotometer was used for UV-Vis absorption spectra and chromaticity diagram measurements (at Marmara University, Turkey). *In-situ* spectroelectrochemical measurements were carried out by utilizing a three-electrode configuration of thin-layer quartz spectroelectrochemical cell consisting a Pt tulle working electrode, a Pt wire counter electrode, and a SCE reference electrode. The spectroelectrochemical cell we used is a homemade cell. Three quartz necks were welded on a quartz fluorescence cuvette which has 2 mm light path. Three quartz necks were used as holder for the electrodes. 2 mm light path of the fluorescence cuvette supply a thin layer for the electroactive species in it. *In-situ* electrocolorimetric measurements, under potentiostatic control, were obtained using an Ocean Optics QE65000 diode array spectrophotometer at color measurement mode by utilizing a three-electrode configuration of thin-layer quartz spectroelectrochemical cell.

2.3. Synthesis

2.3.1. *Preparation of 4-(2-(benzo[d]thiazol-2-yl)phenoxy)phthalonitrile* (**3**)

A solution of 2-(benzo[d]thiazol-2-yl)phenol (**1**) (1 g, 4.4 mmol) and *4*-nitro phthalonitrile (0.76 g, 4.4 mmol) (**2**) in dry DMF (15 mL) was stirred at 50 ^{o}C for 10 min under a nitrogen atmosphere. And then, finely ground anhydrous K_2CO_3 (2.43 g, 17.6 mmol) was added portionwise over a period of 2 h with stirring at this temperature. After stirring for 120 h at 50 ^{o}C, the reaction mixture was poured over crushed ice and the resulting white precipitate was filtered off, washed with distilled water, and then dried *in vacuo*. Yield: 1.5 g

(97 %), m.p.: 177-179 ^{o}C. Calc. for $C_{21}H_{11}N_3OS$: % C 71.37, % H 3.14, % N 11.89. Found: % C 71.39, % H 3.19, % N 11.85. FT-IR ν_{max}/cm^{-1} : 3070 (Ar-H), 2234 (C≡N), 1601, 1561 (C=N), 1485, 1251 (Ar-O-C), 1105, 955, 837, 759, 694 (C-S). ^{1}H NMR ($CDCl_3$) (δ: ppm): 8.60 (ArH, 1H, d), 8.11 (Ar-H, 1H, d), 7.91 (ArH, 1H, d), 7.75 (ArH, 1H, d), 7.53-7.22 (ArH, 7H, m). ^{13}C NMR ($CDCl_3$) (δ: ppm): 161.01, 152.68, 151.14, 135.79, 132.70, 131.30, 127.33, 126.79, 125.91, 123.65, 122.06, 121.87, 121.68, 121.43, 118.12, 115.44, 115.06, 109.92. MALDI-TOF, *m/z*: Calc.: 353.40; Found: 353.12 $[M]^+$.

2.3.2. *Preparation of metal-free phthalocyanine* (**4**)

In dry *n*-pentanol (3 mL), compound **3** (0.3 g, 0.85 mmol) and three drops of 1,8-diazabicyclo[5.4.0]undec-7-ene were stirred under reflux in a nitrogen atmosphere at 160 ^{o}C in a sealed glass tube for 24 h and degassed several times. Thereafter, the reaction mixture was left to cool to the room temperature. With adding ethanol (10 mL), the green crude product was precipitated and filtered off. After the refluxing with ethanol (40 mL) for 4 h, the obtained green product was filtered off again and was successively washed several times with hot ethanol, distilled water and diethyl ether in order to removing the unreacted organic materials. After drying *in vacuo*, it was purified by column chromatography using chloroform-methanol (93:7) solvent system as eluent. Yield: 110 mg (37 %), m.p.:>300 ^{o}C (decomposition). Calc. for $C_{84}H_{46}N_{12}O_4S_4$: % C 71.27, % H 3.28, % N 11.87. Found: % C 71.33, % H 3.36, % N 11.89. FT-IR ν_{max}/cm^{-1}: 3287 (N-H), 3060 (Ar-H), 1610 (N-H, bend.), 1577 (C=N), 1447, 1228 (Ar-O-C), 1089, 925, 752, 692 (C-S). ^{1}H NMR ($CDCl_3$) (δ: ppm): 8.50 (ArH, 4H, m), 8.05 (ArH, 4H, m), 7.37-6.98 (ArH, 36H, m). UV/Vis (THF): λ, nm

(log ε): 700 (5.20), 665 (5.16), 638 (4.81), 605 (4.68), 383 (4.78). MALDI-TOF, *m/z*: Calc.: 1415.63; Found: 1415.57 $[M]^+$.

2.3.3. *General procedures for metallophthalocyanine derivatives* (**5–8**)

The mixture of compound **3** (0.3 g, 0.85 mmol), the related anhydrous metal salt [$Zn(CH_3COO)_2$ (38 mg, 0.21 mmol) for compound **5** , PbO (47 mg, 0.21 mmol) for compound **6**, $CoCl_2$ (27 mg, 0.21 mmol) for compound **7**, $CuCl_2$ (28 mg, 0.21 mmol) for compound **8**] and three drops of 1,8-diazabicyclo[5.4.0]undec-7-ene was heated at 160 ^oC with dry *n*-pentanol (3 mL) in a sealed tube, and stirred for 24 h. Later on , the reaction mixture was left to cool into the room temperature. With adding ethanol (10 mL), the green crude product was precipitated and filtered off. After the refluxing with ethanol (40 mL) for 4 h, the obtained green product was filtered off again and was successively washed several times with hot ethanol, distilled water and diethyl ether in order to removing the unreacted organic materials. After drying *in vacuo*, it was purified by column chromatography using chloroform-methanol ((93:7) for compound **5**, (91:9) for compound **6**, (92:8) for compound **7** and (95:5) for compound **8**, respectively) solvent system as eluent.

2.3.3.1. *Preparation of zinc(II) phthalocyanine* (**5**)

Yield: 83 mg (26 %), m.p.: >300 ^oC (decomposition). Calc. for $C_{84}H_{44}N_{12}O_4S_4Zn$: % C 68.22, % H 3.00, % N 11.36. Found: % C 68.30, % H 3.08, % N 11.32. FT-IR ν_{max}/cm^{-1} : 3059 (Ar-H), 1717, 1610 (C=N), 1448, 1316, 1229 (Ar-O-C), 1042, 941, 833, 746, 692 (C-S). ^1H NMR ($CDCl_3$) (δ: ppm): 8.92 (ArH, 8H, m), 7.93 (ArH, 8H, m), 7.36 (ArH, 28H, m). UV/Vis

(THF): λ, nm (log ε): 673 (5.30), 607 (4.63), 356 (4.96), 328 (5.02). MALDI-TOF, *m/z*: Calc.: 1479.01; Found: 1479.40 $[M+]^+$.

2.3.3.2. *Preparation of lead(II) phthalocyanine* (**6**)

Yield: 132 mg (38 %), m.p.:>300 ^oC (decomposition). Calc. for $C_{84}H_{44}N_{12}O_4S_4Pb$: % C 62.25, % H 2.74, % N 10.37. Found: % C 62.28, % H 2.81, % N 10.35. FT-IR ν_{max}/cm^{-1}: 3058 (Ar-H), 1604 (C=N), 1447, 1317, 1229 (Ar-O-C), 1077, 939, 824, 754, 692 (C-S). ^1H NMR ($CDCl_3$) (δ: ppm): 9.10 (ArH, 6H, m), 8.59 (ArH, 4H, m), 7.43 (ArH, 34H, m). UV/Vis (THF): λ, nm (log ε): 707 (5.29), 638 (4.60), 363 (4.87). MALDI-TOF, *m/z*: Calc.: 1620.82; Found: 1619.96 $[M-H]^+$.

2.3.3.3. *Preparation of cobalt(II) phthalocyanine* (**7**)

Yield: 68 mg (22 %), m.p.: >300 ^oC (decomposition). Calc. for $C_{84}H_{44}CoN_{12}O_4S_4$: % C 68.52, % H 3.01, % N 11.41. Found: % C 68.49, % H 3.09, % N 11.35. FT-IR ν_{max}/cm^{-1}: 3059 (Ar-H), 1610 (C=N), 1448, 1230 (Ar-O-C), 1091, 1055, 955, 825, 751, 692 (C-S). UV/Vis (THF): λ, nm (log ε): 667 (5.26), 601 (4.64), 354 (4.91), 313 (5.21). MALDI-TOF, *m/z*: Calc.: 1472.55; Found: 1473.67 $[M+H]^+$.

2.3.3.4. *Preparation of copper(II) phthalocyanine* (**8**)

Yield: 150 mg (48 %), m.p.: >300 ^oC (decomposition). Calc. for $C_{84}H_{44}CuN_{12}O_4S_4$: % C 68.30, % H 3.00, % N 11.38. Found: % C 68.37, % H 3.06, % N 11.43. FT-IR ν_{max}/cm^{-1}: 3060 (Ar-H), 1610 (C=N), 1447, 1317, 1229 (Ar-O-C), 1090, 947, 876, 753, 691 (Ar-O-C).

UV/Vis (THF): λ, nm (log ε): 675 (5.29), 608 (4.75), 348 (4.94). MALDI-TOF, *m/z*: Calc.: 1477.16; Found: 1478.36 $[M+H]^+$.

3. Results and discussion

The general synthetic route for the synthesis of new dinitrile compound and phthalocyanines is given in Scheme 1. The precursor material chosen for the synthesis of tetra-substituted phthalocyanine derivatives (**4-8**) on the peripherally is *4-(2-(benzo[d]thiazol-2-yl)phenoxy)phthalonitrile* (**3**). Compound **3** has been prepared by K_2CO_3 catalyzed nucleophilic substitution of the nitro group in *4*-nitro phthalonitrile (**2**) with 2-(benzo[d]thiazol-2-yl)phenol (**1**) according to reported procedure [42]. *4-(2-(benzo[d]thiazol-2-yl)phenoxy*-substituted **H_2Pc** (**4**) is prepared by cyclotetramerization of *4-(2-(benzo[d]thiazol-2-yl)phenoxy)phthalonitrile* (**3**) in the presence of 1,8-diazabicyclo[5.4.0]undec-7-ene, in dry *n*-pentanol at 160 ^oC for 24 h with the yield of 37 %. Tetra-substituted **ZnPc (5), PbPc (6), CoPc (7)** and **CuPc (8)** compounds are also obtained by cyclotetramerization of *4-(2-(benzo[d]thiazol-2-yl)phenoxy)phthalonitrile* (**3**) in the presence of related metal salts ($Zn(CH_3COO)_2$, (PbO), $CoCl_2$ and $CuCl_2$) and two drops of 1,8-diazabicyclo[5.4.0]undec-7-ene in dry *n*-pentanol 160 ^oC for 24 h with the yields of 26, 38, 22 and 48 % (for compounds **5-8**), respectively. All novel phthalocyanines were purified on silica gel by column chromatography using chloroform: methanol [(93:7), (91:9), (92:8) and (95:5)] solvent system as eluent.

Although phthalocyanine complexes have low solubility in most organic solvents, adding the some substituents on the phthalocyanine core increases the solubility. All synthesized phthalocyanine derivatives (**4-8**) exhibit excellent solubility in most organic solvents (e.g. chloroform, dichloromethane, THF, DMSO and DMF). These organo-soluble

phthalocyanines (**4-8**) have been characterized by several spectral methods for supporting the formation of the molecules.

In FT-IR spectrum of compound **3**, the characteristic C≡N stretch was observed at ~2234 cm^{-1}. However, the cyclotetramerization of the dinitrile derivative (**3**) to the **H_2Pc**(**4**) and MPcs (**5-8**) was confirmed by the disappearance of the intense C≡N vibration at ~2234 cm^{-1}.

In the ^{1}H NMR spectrum of compound **3** in deuterated $CDCl_3$, aromatic protons were observed at *δ*: 8.60 (d), 8.11 (d), 7.91 (d), 7.75 (d) and 7.53-7.22 (m) (Fig. S1). For the tetra-substituted **H_2Pc** (**4**), the resonances belonging to the aromatic protons were observed at *δ*: 8.50 (m), 8.05 (m), 7.37-6.98 (m). The typical shielding of inner core protons belonging to the **H_2Pc** (**4**), which are generally shown at the negative ppm region [43], were not observed because of strong aggregation [44]. In the ^{1}H NMR spectra of **ZnPc (5)** and **PbPc (6)**, the aromatic protons were observed at between *δ*: 8.92-7.36 ppm for **ZnPc (5)** and *δ*: 9.10-7.43 ppm for **PbPc (6)**, respectively. Because of their paramagnetic nature, ^{1}H NMR of the **CoPc (7)** and **CuPc (8**) derivatives was precluded.

In the ^{13}C NMR spectrum of compound **3**, the characteristic peaks belonging to dicyano carbon atoms were observed at *δ*: 115.44 and 115.06 ppm, as expected (Fig. S2).

In the mass spectra of compounds **3**, the presence of molecular ion peak at m/z: 353.12 $[M]^+$ confirmed the purposed structure (Fig. S3). The molecular ion peaks which were observed at m/z: 1415.57 $[M]^+$ for **H_2Pc** (**4**), 1479.40 $[M]^+$ for **ZnPc (5)**, 1619.96 $[M-H]^+$ for **PbPc (6)**, 1473.67 $[M+H]^+$ for **CoPc (7)** and 1478.36 $[M+H]^+$ for **CuPc (8)**, supported the desired structures (Fig. S3 and Fig. S4). In addition to these data, the elemental analysis of those compounds was also determined.

3.1. Electronic absorption spectra

Fig. 1 shows typical UV/Vis absorption spectra of **H_2Pc** (**4**), **ZnPc** (**5**), **PbPc** (**6**), **CoPc** (**7**) and **CuPc** (**8**) derivatives in THF. Generally, phthalocyanines and their derivatives exhibit UV/Vis spectra with two intense absorption regions around approximately 300-400 nm (B-band) and around 600-700 nm (Q-band). The Q-band is due to the transition from the ground state of A_{1g} symmetry to the first excited state which is of E_u symmetry. The splitting of Q-band is because of the lifting of degeneracy of LUMO to a varying extent [45].

The absorption spectrum of H_2Pc (**4**) includes a splitting intense Q-band near at λ_{max}: 700 and 665 nm with shoulders at λ_{max}: 638 and 605 nm and the B-band at λ_{max}: 383 nm (Table 1). In the UV/Vis spectrum of **H_2Pc (4)**, the Q band splitting has been interpreted due to the diagonally occupying two protons on the pyrrolic nitrogens reducing the molecular symmetry from D_{4h} to D_{2h} [46]. For compound **5-8**, the Q-bands were observed at λ_{max}: 673, 707, 667 and 675 nm with shoulders λ_{max}: 607, 638, 601 and 608 nm, respectively. The B-bands were observed at (356, 328), 363, 313 and 348 nm for compounds **5-8**, respectively (Table 1). In absorption spectra, **PbPc (6**) was redshifted compared to **H_2Pc** (**4**) and MPcs (**5**, **7**, **8**). The large redshift was attributed to highly deformed phthalocyanine skeleton due to the central metals which was not fitting into the cavity of phthalocyanine molecule. Namely, deformation of phthalocyanine ligand results in the redshifting of the Q-band [45].

3.2. Voltammetric Measurements

Redox behaviors of the complexes were performed in DCM/TBAP electrolyte system on a Pt working electrode with cyclic voltammetry (CV) and square wave voltammetry (SWV) to support the proposed structure of the complexes and to decide possible

applications. All redox processes were analyzed and derived voltammetric parameters were tabulated on Table 2.

Fig. 2 shows CV responses of **H_2Pc** (**4**). It displays two reversible reduction reactions labeled as **R_1** ($E_{1/2}$ = -0.62 V;ΔE_p= 59 mV; I_{pa}/I_{pc} = 0.98) and **R_2** ($E_{1/2}$ = -0.91 V;ΔE_p = 60 mV; I_{pa}/I_{pc} = 0.96) and two oxidation couples labeled as **O_1** ($E_{1/2}$ = 0.92 V;ΔE_p = 65 mV; I_{pa}/I_{pc} = 0.93) and **O_2** ($E_{1/2}$ = 1.12 V; ΔE_p = 72 mV; I_{pa}/I_{pc} = 0.91). All electron transfer processes are both electrochemically and chemically reversible with respect to ΔE_p and I_{pa}/I_{pc} values. SVWs of the complex clearly support these reversible characters of the processes, since these couples show symmetric anodic and cathodic peaks with the same peak currents (Fig. 2b). **H_2Pc** (**4**) has 1.54 V $\Delta E_{1/2}$ (separation between first anodic and first cathodic peak), which directly expresses the HOMO-LUMO gap of the complex. When compared with the similar complexes in the literature, redox couples shift to positive potentials due to the electron releasing 4-(2-(benzo[d]thiazol-2-yl)phenoxy) groups. HOMO-LUMO gap of the complex is in a great harmony with the metal free phthalocyanines in the literature [47-49].

As shown in Fig. 3, **ZnPc** (**5**) gives a reversible oxidation (**O_1** at 0.75 V) during the anodic scans. However cathodic peaks are complicated with the aggregation of the complex. First reduction process splits into two waves, R'_1 for aggregated species at -0.87 V and R_1 for monomeric species at -1.01 V at 0.100 Vs^{-1} scan rate. This reduction process is followed with the second quasi-reversible reduction process R_2 at -1.30 V (ΔE_p = 130 mV; I_{pa}/I_{pc} = 0.75). When compared with the redox responses of **H_2Pc** (**4**), electron transfer processes of **ZnPc** (**5**) shifts to the negative potentials. These potential differences are resulted from the effective nuclear charge differences between the 2H and Zn centers of the Pc rings [47-52].

The radius of divalent lead ions (1.75 Å) in the core of PbPc is greater than the radius of the inner core, so the metal ion does not fit inside the central cavity but it lies out of the phthalocyanine plane [53-55]. Therefore, the complex shows a demetallization tendency in

the redox reactions. Therefore, these compounds show anomalous redox behaviors together with tuning the physicochemical properties of MPc [56, 57]. Fig. 4 shows the voltammetric responses of **PbPc** (**6**). **PbPc** (**6**) gives very similar redox responses with those of **H_2Pc** (**4**). It displays two reversible reduction reactions labeled as **R_1** ($E_{1/2}$ = -0.61 V;ΔE_p= 80 mV; I_{pa}/I_{pc} = 0.95) and **R_2** ($E_{1/2}$ = -0.94 V;ΔE_p = 90 mV; I_{pa}/I_{pc} = 0.90) and two oxidation couples labeled as **O_1** ($E_{1/2}$ = 0.83 V;ΔE_p = 110 mV; I_{pa}/I_{pc} = 0.83) and **O_2** ($E_{1/2}$ = 1.33 V;ΔE_p = 85 mV; I_{pa}/I_{pc} = 0.55). Although **H_2Pc** (**4**) gives completely reversible couples, redox reactions of **PbPc** (**6**) have quasi-reversible peak characters. Especially O_2 couple of **PbPc** (**6**) is chemically irreversible. The reversibility of the complex was also checked with the SWV given in Fig. 4b. Peak current ratios and symmetry of the peaks of a redox couple were used to characterize reversibility or irreversibility of a redox process. In our previous papers, we illustrated the redox responses of PbPc complexes [58-61]. Although demetallation of the **PbPc** complexes during the cathodic potential scans were observed, **PbPc** (**6**) studied here gives a stable redox responses without a chemical reaction, which illustrate stabilization of the Pb center with the effect of 4-(2-(benzo[d]thiazol-2-yl)phenoxy) substituents.

CoPc (**7**) has different voltammetric responses than those of **H_2Pc** (**4**), **ZnPc** (**5**) and **PbPc** (**6**). Since while **H_2Pc** (**4**), **ZnPc** (**5**) and **PbPc** (**6**) represent only Pc based electron transfer reactions, **CoPc** (**7**) gives a metal based reduction process in addition to the Pc based electron transfer reactions. As shown in Fig. 5, an irreversible R_1 at -0.05 V assigned to the reduction of monomeric CoPc ($Co^{II}Pc^{-2}/Co^{I}Pc^{-2}$) and an irreversible R'_1 at -0.55 V assigned to the reduction of aggregated CoPc ($[Co^{II}Pc^{-2}]_{agg}/ [Co^{I}Pc^{-2}]_{agg}$). Redox responses of the complex recorded at different concentration and at different scan rates indicate the aggregation of the complex. At higher concentrations, the current of the peak assigned to the aggregated CoPc ($[Co^{II}Pc^{-2}]_{agg}/ [Co^{I}Pc^{-2}]_{agg}$ increased more than those assigned to the monomeric CoPc ($Co^{II}Pc^{-2}/Co^{I}Pc^{-2}$) species. These voltammetric behavior indicate presence of an equilibrium between

$[Co^{II}Pc^{-2}]_{agg}$ and monomeric CoPc. At faster scan rates the aggregation peak R'_1 at -0.55 V observed more clearly and this peak disappeared at the slow scan rates as shown in Fig. 5. These behaviors support the aggregation phenomena of the complex. This metal based reduction processes are followed with a quasi-reversible Pc ring based reduction process, R_2 at -1.31 V. A Pc based oxidation reaction having reversible peak character is also recorded at 0.78 V during the anodic potential scans. Peak assignments and aggregation properties of the complex were supported with the *in situ* spectroelectrochemical measurements given below. Electrochemical behaviors of CoPc is in a good agreement with the similar CoPc complexes reported in the literature [62-65], which support the proposed structure of the complex synthesized here. CoPc complexes generally give a metal based reduction process at around 0 V due to the electron gaining to the empty d orbitals of Co^{II} center located between the HOMO and LUMO orbitals of Pc ring in noncoordinating solvents like DCM. Separation of around 1 V between the metal based and ring based reduction process is a characteristic response of CoPc complexes.

3.3. Spectroelectrochemistry

Spectroelectrochemical studies were employed to confirm the assignments of the redox couple recorded in the CVs and SWVs of the complexes. Fig. 6 represents *in situ* recorded UV-Vis spectral changes and *in situ* recorded chromaticity diagram of **H_2Pc** (**4**) under applied potentials of the electron transfer reactions. **H_2Pc** (**4**) gives a split Q band at 673 and 710 nm with the shoulders at 611 and 642 nm at 0.0 V applied potential. When -0.85 V was applied to the working electrode, the split Q band turn to a single band at 675 nm as a result of increasing a sharp band. These spectral changes are characteristic changes for the first reduction reaction of metal free phthalocyanines (Fig. 6a) [47-49, 66, 67]. During the

second reduction reaction, while the Q band at 675 nm decreases, the region at around 500 nm increases in intensity, which characterizes the reduction of the monoanionic form of **H_2Pc** species (Fig. 6b). Fig. 6c illustrates the spectral changes of **H_2Pc** (**4**) during the first oxidation reaction. The split Q bands decrease in intensity and the region at around 500 nm starts to increases first of all. But then all bands decrease in intensity due to the decomposition of the oxidized form of the complex. Color of the electrogenerated forms of the complex was recorded with *in situ* chronocolorimetry, however a distinctive color change was not recorded between the electrogenerated forms of the complex.

Spectroelectrochemical results of **ZnPc** (**5**) were consistent with the Pc ring based reduction of the MPcs having redox inactive metal centers. However spectroelectrochemical studies of **PbPc** (**6**) indicate different spectroscopic changes than the common ring based redox processes due to the demetallization of the complexes. Fig. 7 and 8 illustrate the *in situ* spectroelectrochemical and *in situ* electrocolorimetric results of **PbPc** (**6**) under the applied potential of the redox processes. Under –0.75 V potential application, first of all, while the Q band at 717 nm starts to decreases, a new band increases at 677 nm and a split Q band is formed (Fig. 7a). The final spectrum in the Fig. 7a (blue spectrum) is a characteristic spectrum for the metal-free phthalocyanine. Thus these spectral changes are easily assigned to the demetallation of **PbPc** (**6**) and formation of **H_2Pc** (**4**). At the same potential application, the band at 717 nm disappears, while the band at 677 nm increases in intensity. These spectral changes are similar changes with the reduction of metal free phthalocyanine (Fig. 7b). Fig. 7c illustrates the spectral changes under -1.30 V. These spectral changes are characteristic changes for the ring based reduction of MPc complexes. While the Q band at 677 nm decreases in intensity, a new band is recorded at 540 nm. Decreasing of the Q band without shifting and observation of a new band between 500 and 600 nm characterize a Pc based reduction process [52, 58-61, 68]. In our previous studies [58-61], we also indicated the

demetallization of the PbPcs before or after the first reduction processes and during the positive potential scans depending on the substituents. Fig. 8a represents the spectral changes during the first oxidation reaction. While the Q band at 717 nm decreases in intensity, two new bands are recorded at MLCT (Metal to Ligand Charge Transfer) regions (at 536 and 884 nm). These spectral changes are characteristic changes for the ring based oxidation of MPc complexes. All bands decrease in intensity due to the decomposition as shown in Fig. 8b during the second oxidation reaction. This decomposition reaction is recorded with the CV and SWV measurements as shown in Fig. 4. The green color of the solution (point □ x=0.3068, y=0.3605) changes to greenish yellow (point ☆ x=0.352, y=0.3553) during the first oxidation process (Fig. 7d) and to the blue (point △ x=0.3151, y=0.3164) after the second reduction reaction.

CoPc (**7**) has different voltammetric responses then the others, which also differs the spectral changes recorded during the *in situ* spectroelectrochemical measurements. While **H_2Pc** (**4**)**, ZnPc** (**5**) and **PbPc** (**6**) complexes give spectral changes assigned to the Pc ring based electron transfer processes, **CoPc** (**7**) illustrates spectral changes assigned to the metal based reduction reaction during the first reduction reaction (Fig. 9). When -0.75 V was applied, the Q band at 674 nm decreases in intensity and a small band is observed at 643 nm, which assigned to the aggregation of the **CoPc** (**7**). And then while the Q band decreases and a new Q band is recorded at 706 nm. At the same time a sharp band is recorded at 474 nm. Totally while the Q band shifts from 674 nm to 706 nm, a new band is recorded at 474 nm (Fig. 9a). Shifting of the Q band and observation of a new band between 450 and 500 nm characterizes the reduction of $Co^{II}Pc^{-2}$ to $Co^{I}Pc^{-2}$ species [69-74]. Fig. 9b illustrates the spectral changes during the oxidation reaction. Decreasing of the Q band at 674 nm, and observation of a new band at 505 nm characterize the Pc based oxidation of the complex.

Chromaticity diagram in Fig. 9c represents the color of the electrogenerated species of the complex.

4. Conclusions

In this study, the synthesis of novel peripherally tetra-*4-(2-(benzo[d]thiazol-2-yl)phenoxy)*substituted **H_2Pc (4), ZnPc (5), PbPc (6), CoPc (7)** and **CuPc (8**) compounds were described and characterized by using different spectroscopic techniques (e.g. FT-IR, ^{1}H NMR, ^{13}C NMR, elemental analysis, mass spectroscopy, UV/Vis spectral data) for the first time. In the UV-Vis spectra, while the **H_2Pc** (**4**) shows splitting Q band, the metallophthalocyanines (**5-8**) exhibit single narrow Q bands as expected and support the formation of phthalocyanine complexes in THF.

Electrochemical and spectroelectrochemical measurement support the proposed structure of the complexes. **H_2Pc** (**4**) and **ZnPc** (**5**) illustrate the common Pc based electron transfer reactions. Redox responses **ZnPc** (**5**) and **CoPc** (**7**) complicated generally with the aggregation of the complexes. Although **PbPc** (**6**) gives clear well defined reversible reduction and oxidation reactions during the CV and SWV measurements, it demetallized during the *in situ* spectroelectrochemical reaction. **CoPc** (**7**) represents a metal based reduction reaction, while the others give ring based reduction reactions. Redox richness of the complexes illustrates their possible usage in different electrochemical technologies, such as electrocatalytic, electrosensing and electrochromic fields. Especially different color of the electrochemically generated redox species recorded during the *in situ* spectroelectrochemical measurements indicates their suitability in the displaying technologies.

Acknowledgement

This study was supported by the Research Fund of Karadeniz Technical University, Project no: 2010.111.002.1 (Trabzon-Turkey). We thank to The Turkish Academy of Sciences (TUBA) for their financial support.

References

[1] J.H. Zagal, F. Bedioui, J.P. Dodelet, N4-Macrocyclic metal complexes, Springer Science-Business Media, New York, USA, 2006.

[2] Y. Zhang, X. Cai, Y. Bian, J. Jiang, Organic semiconductors of phthalocyanine compounds for field effect transistors (FETs), Struct. Bond. 135 (2010) 275-322.

[3] A.L. Thomas, Phthalocyanine research and applications, CRC Press, Boca Raton, Florida, 1990.

[4] P. Erk, H. Hengelsber, The porphyrin handbook, in: K.M. Kadish, K.M. Smith, R. Guilard (Eds), Applications of phthalocyanines, Vol.19, Academic Press, San Diego, California, 2003.

[5] Ö. Bekaroğlu, Ball-type phthalocyanines: synthesis and properties, Struct. Bond. 135 (2010)105-136.

[6] F. Yakuphanoglu, M. Durmuş, M. Okutan, O. Köysal, V. Ahsen, The refractive index dispersion and the optical constants of liquid crystal metal-free and nickel(II) phthalocyanines, Physica B 373 (2006) 262-266.

[7] Y.H. Gursel, B.F. Senkal, M. Kandaz, F. Yakuphanoglu, Synthesis and liquid crystal properties of phthalocyanine bearing a star polytetrahydrofuran moiety, Polyhedron 28 (2009)1490-1496.

[8] H. Xia, M. Nogami, Copper phthalocyanine bonding with gel and their optical properties, Opt Mater 15 (2000)93-98.

[9] S. Makhseed, M. Al-Sawah, J. Samuel, H. Manaa, Synthesis, characterization and nonlinear optical properties of nonaggregating hexadeca-substituted phthalocyanines, Tetrahedron Lett. 50 (2009)165-168.

[10] Y.S. Krasnov, G.Y. Kolbasov, I.N. Tretyakova, L.A. Tomachynska, V.Y. Chernii, S.V. Volkov, Dynamics of redox processes and electrochromism of films of zirconium (IV) phthalocyanines with out-of-plane β-dicarbonyl ligands, Solid State Ionics 180 (2009) 928-933.

[11] P.M.S. Monk, R.J. Mortimer, D.R. Rosseinsky. Electrochromism: Fundamentals and applications, VCH Publishers, Weinehim, 1995.

[12] T.V. Basova, C. Taşaltin, A.G. Gürek, M.A. Ebeoğlu, Z.Z. Öztürk, V. Ahsen, Mesomorphic phthalocyanine as chemically sensitive coatings for chemical sensors, Sensor Actuat. B-Chem. 96 (2003)70-75.

[13] L. Valli, Phthalocyanine-based Langmuir–Blodgett films as chemical sensors, Adv. Colloid. Interfac. 116 (2005)13-44.

[14] M. Bouvet, Phthalocyanine-based field-effect transistors as gas sensors, Anal. Bioanal. Chem. 384 (2006)366-373.

[15] A. Moussaron, J.S. Thomann, R. Vanderesse, P. Arnoux, M. Barberi-Heyob, G. Creusat, P. Boisseau, C. Frochot, Synthesis of phthalocyanines (Pcs) for photodynamic therapy (PDT), Photodiagn. Photodyn. 8 (2011)193-194.

[16] L.M. Moreira, F.V. dos Santos, J.P. Lyon, M. Maftoum-Costa, C. Pacheco-Soares, N.S. da Silva, Photodynamic therapy: Porphyrins and phthalocyanines as photosensitizers, Aust. J. Chem. 61 (2008)741-754.

[17] M.P. De Filippis, D. Dei, L. Fantetti, G. Roncucci, Synthesis of a new water-soluble

octa-cationic phthalocyanine derivative for PDT, Tetrahedron Lett. 41 (2000) 9143-9147.

[18] J.A. Carruth , Clinical applications of photodynamic therapy, Int. J. Clin. Pract. 52 (1998) 39-42.

[19] J. Huang, N. Chen, J. Huang, E. Liu, J. Xue, S. Yang, Z. Huang, J. Sun, Metal phthalocyanine as photosensitizer for photodynamic therapy (PDT). Preparation, characterization and anticancer activities of an amphiphilic phthalocyanine $ZnPcS_2P_2$, Sci. China Ser. B. 44 (2001)113-122.

[20] T.J. Dougherty , C.J. Gomer , B.W. Henderson , G. Jori , D. Kessel , M. Korbelik , J. Moan , Q. Peng , Photodynamic therapy, J. Natl. Cancer I. 17, 90 (1998) 889-905.

[21] J. Mack, M.J. Stillman, The porphrin handbook, in: K.M. Kadish, K.M. Smith, R. Guilard (Eds), Phthalocyanines, spectroscopic and electrochemical characterization, Vol. 16, Academic Press, San Diego, California, 2003.

[22] M. Durmuş, T. Nyokong, Synthesis, photophysical and photochemical properties of tetra- and octa-substituted gallium and indium phthalocyanines, Polyhedron 26 (2007) 3323-3335.

[23] J.V. Metzger, The Chemistry of Heterocyclic Compounds, John Wiley&Sons Inc, Canada, 1979.

[24] H. Y. Yenilmez, A. M. Sevim, Z. A. Bayır, Synthesis and photophysics of new metallo phthalocyanine complexes with thiazole groups and their fluorescence quenching studies with benzoquinone, Synthetic Met. 176 (2013) 11-17.

[25] İ. Değirmencioğlu, E. Atalay, M. Er, Y. Köysal, Ş. Işık, K. Serbest, Novel phthalocyanines containing substituted salicyclic hydrazone-1,3-thiazole moieties: Microwave-assisted synthesis, spectroscopic characterization, X-ray structure and thermal characterization, Dyes Pigments 84 (2010) 69-78.

[26] G. Dede, R. Bayrak, M. Er, A.R. Özkaya, İ. Değirmencioğlu, DBU-catalyzed condensation of metal free and metallophthalocyanines containing thiazole and azine moieties: Synthesis, characterization and electrochemical properties, J Organomet Chem 740 (2013) 70-77.

[27] X. Zuo, H. Zhang, N. Li, An electrochemical biosensor for determination of ascorbic acid by cobalt (II) phthalocyanine–multi-walled carbon nanotubes modified glassy carbon electrode, Sensor Actuat. B-Chem. 161 (2012)1074-1079.

[28] P. Kalimuthu, A. Sivanesan, S.A. John, Fabrication of optochemical and electrochemical sensors using thin films of porphyrin and phthalocyanine derivatives, J. Chem. Sci. 124 (2012)1315-1325.

[29] B. Ceken, M. Kandaz. A. Koca, Electrochemical metal-ion sensors based on a novel manganese phthalocyanine complex, Synthetic Met. 162 (2012)1524-1530.

[30] E.F. Perez, G.D. Neto, A.A. Tanaka, L.T. Kubota, Electrochemical sensor for hydrazine based on silica modified with nickel tetrasulfonated phthalocyanine, Electroanal. 10 (1998)111-115.

[31] K. Shinbo, K. Kato, F. Kaneko, K. Onishi, R.C. Advincula, X. Fan, R.C. Advincula, Fabrication and electrochromic properties of layer-by-layer self-assembled ultrathin films containing water-soluble phthalocyanine, Mol. Cryst. Liq. Cryst. 407 (2003) 493-500.

[32] C.L. Lin, C.C. Lee, K.C. Ho, Spectroelectrochemical studies of manganese phthalocyanine thin films for applications in electrochromic devices, J. Electroanal. Chem. 524 (2002) 81-89.

[33] J. Silver, P. Lukes, A. Houlton, P. Hey, M.T. Ahmet, Electrochromism in the transition-metal phthalocyanines.4. Complementary colors in cobalt phthalocyanine films during electrochromic cycling, Int. J. Electron. 77 (1994) 155-171.

[34] S. Vilakazi, T. Nyokong, T. Fukuda, N. Kobayashi, Electrocatalytic behavior of cobalt phthalocyanine complexes immobilized on glassy carbon electrode towards the reduction of dicrotophos pesticide, J. Porphyr. Phthalocya. 16 (2012) 939-945.

[35] A. Koca, A. Kalkan, Z.A. Bayir, Electrocatalytic oxygen reduction and hydrogen evolution reactions on phthalocyanine modified electrodes: Electrochemical, *in situ* spectroelectrochemical, and *in situ* electrocolorimetric monitoring, Electrochim. Acta 56 (2011) 5513-5525.

[36] I. Balan, I.G. David, V. David, A.I. Stoica, C. Mihailciuc, I. Stamatin, A.A. Ciucu, Electrocatalytic voltammetric determination of guanine at a cobalt phthalocyanine modified carbon nanotubes paste electrode, J. Electroanal. Chem. 654 (2011) 8-12.

[37] D. Wohrle, G. Schnurpfeil, S. Makarov, O. Suvorova, Der Weg von Farbstoffen/Pigmenten zu Materialien für optische, elektronische und photoelektronische Bauelemente, Chem. Unserer. Zeit. 46 (2012)12-24.

[38] G. Giancane, T. Basova, A. Hassan, G. Gumus, A.G. Gurek, V. Ahsen, L. Valli, Investigations and application in piezoelectric phenol sensor of Langmuir–Schäfer films of a copper phthalocyanine derivative functionalized with bulky substituents, J. Colloid. Interf. Sci. 377 (2012)176-183.

[39] M. Camur, M. Bulut, M. Kandaz, O. Guney, Effects of coumarin substituents on the photophysical properties of newly synthesised phthalocyanine derivatives, Supramol. Chem. 21 (2009) 624-631.

[40] D.D. Perrin, W.L.F. Armarego, Purification of laboratory chemicals, 2nd ed. Pergamon Press, Oxford, 1989.

[41] J.G. Young, W. Onyebuagu, Synthesis and characterization of di-disubstituted phthalocyanines, J. Org. Chem. 55 (1990) 2155-2159.

[42] T. Ceyhan, Ö. Bekaroğlu,The synthesis of new phthalocyanine substituted with 12-

membered diazadioxa macrocycles, Monatsh. Chem. 133 (2002) 71-78.

[43] S. Dabak, Ö. Bekaroğlu, Synthesis of phthalocyanines crosswise-substituted with two alkylsulfanyl and two amino groups, New. J. Chem. 21 (1997) 267-271.

[44] H. Kantekin, M. Rakap, Y. Gök, H.Z. Şahinbaş, Synthesis and characterization of new metal-free and phthalocyanine nickel (II) complex containing macrocyclic moieties, Dyes Pigments 74 (2007) 21-25.

[45] T. Nyokong, Electronic spectral and electrochemical behavior of near infrared absorbing metallophthalocyanines, Struct. Bond. 135 (2010) 45-88.

[46] K.M. Kadish, K.M. Smith, R. Guilard (Eds), Handbook of porphyrin science: with applications to chemistry, physics, materials science, engineering, biology and medicine, Vol.9, Electronic absoption spectra-phthalocyanines, Word Scientific Publishing, Singapore, 2010.

[47] I. Cince, A.R. Ozkaya, Electrochemical reduction and oxidation of copper, lead complex and metal-free phthalocyanine, Asian J. Chem. 23 (2011) 983-991.

[48] R.J. Li, D.D. Qi, J.Z. Jiang, Y.Z. Bian, Benzo-fused low symmetry metal-free tetraazaporphyrin and phthalocyanine analogs: synthesis, spectroscopy, electrochemistry, and density functional theory calculations, J. Porphyr. Phthalocya. 14 (2010) 421-437.

[49] I. Acar, Z. Biyiklioglu, A. Koca, H. Kantekin, Synthesis, electrochemical, in situ spectroelectrochemical and in situ electrocolorimetric characterization of new metal-free and metallophthalocyanines substituted with 4-{2-[2-(1-naphthyloxy)ethoxy]ethoxy} groups, Polyhedron 29 (2010) 1475-1484.

[50] G.K. Karaoglan, G. Gumrukcu, A. Koca, A. Gul, The synthesis, characterization, electrochemical and spectroelectrochemical properties of a novel, cationic, water-soluble Zn phthalocyanine with extended conjugation, Dyes Pigments 88 (2011) 247-

256.

[51] J. Obirai, T. Nyokong, Synthesis, spectral and electrochemical characterization of mercaptopyrimidine-substituted cobalt, manganese and Zn (II) phthalocyanine complexes, Electrochim Acta. 50 (2005) 3296-3304.

[52] N. Kobayashi, T. Ashida, T. Osa, Synthesis, spectroscopy, electrochemistry, and spectroelectrochemistry of a zinc phthalocyanine with D_{2h} symmetry, Chem. Lett. 21 (1992) 2031-2034.

[53] H. Yamane, H. Honda, H. Fukagawa, M. Ohyama, Y. Hinuma, S. Kera, K.K. Okudaira, N. Ueno, HOMO-band fine structure of OTi- and Pb-phthalocyanine ultrathin films: effects of the electric dipole layer, J. Electron. Spectrosc. 137 (2004) 223-227.

[54] R.A. Collins, A. Krier, A.K. Abass, Optical properties of lead phthalocyanine (PbPc) thin films, Thin Solid Films 229 (1993) 113-118.

[55] H. Hobert, R.C. Weaver, J.D. Wright, Zersetzung von Blei-Phthalocyanin durch Stickstoffdioxid, Zeitschrift für Chemie. 29 (1989) 454-455.

[56] D.K. Modibane, T. Nyokong, Synthesis, photophysical and nonlinear optical properties of microwave synthesized 4-tetra and octa-substituted lead phthalocyanines, Polyhedron 28 (2009)1475-1480.

[57] D.K. Modibane, T. Nyokong, Synthesis and photophysical properties of lead phthalocyanines, Polyhedron 27 (2008) 1102-1110.

[58] A. Gunsel, M.N. Yarasir, M. Kandaz, A. Koca, Synthesis, *H*- or *J*-type aggregations, electrochemistry and *in situ* spectroelectrochemistry of metal ion sensing lead(II) phthalocyanines, Polyhedron 29 (2010) 3394-3404.

[59] H.A. Dincer, M.K. Sener, A. Koca, A. Gul, M.B. Kocak, Synthesis, electrochemistry and in situ spectroelectrochemistry of soluble lead phthalocyanines, Electrochim. Acta

53 (2008) 3459-3467.

[60] M.N. Yarasir, A. Koca, M. Kandaz, B. Salih, Voltammetry and spectroelectrochemical behavior of a novel octapropylporphyrazinato lead(II) complex, J. Phys. Chem. C 111 (2007) 16558-16563.

[61] A. Koca, H.A. Dincer, M.B. Kocak, A. Gul, Electrochemical characterization of Co(II) and Pd(II) phthalocyanines carrying diethoxymalonyl and carboxymethyl substituents, Russ. J. Electrochem+. 42 (2006) 31-37.

[62] K. Sakamoto, E. Ohno, Electrochemical characterization of soluble cobalt phthalocyanine derivatives, Dyes Pigments 37 (1998) 291-306.

[63] M.I. Bazanov, O.V. Shishkina, V.E. Maizlish, A.V. Petrov, G.P. Shaposhnikov, R.P. Smirnov, A. Gzheidzyak, Electrochemical studies of cobalt-containing phthalocyanine compounds, Russ. J. Electrochem+. 34 (1998) 818-821.

[64] B. Ortiz, S.M. Park, N. Doddapaneni, Electrochemical and spectroelectrochemical studies of cobalt phthalocyanine polymers, J. Electrochem. Soc. 143 (1996) 1800-1805.

[65] R. Adzic, B. Simicglavaski, E. Yeager, VI. Voltammetric studies of the adsorbed phthalocyanines on single-crystal silver electrodes, J. Electroanal. Chem. 194 (1985) 155-163.

[66] K.R. Pichaandi, H. Jacobsen, M.J. Fink, INOR 76-Electrochemistry and spectroelectrochemistry of a silicon (IV) phthalocyanine chloride, Abstr. Pap. Am. Chem. S. 235 (2008).

[67] S. Arslan, I .Yilmaz, A new water-soluble metal-free phthalocyanine substituted with naphthoxy-4-sulfonic acid sodium salt. Synthesis, aggregation, electrochemistry and in situ spectroelectrochemistry, Polyhedron 26 (2007) 2387-2394.

[68] A. Koca, H.A. Dincer, H. Cerlek, A. Gul, M.B. Kocak, Spectroelectrochemical

characterization and controlled potential chronocoulometric demetallation of tetra- and octa-substituted lead phthalocyanines, Electrochim. Acta 52 (2006) 1199-1205.

[69] M. Arici, D. Arican, A.L. Ugur, A. Erdogmus, A. Koca, Electrochemical and spectroelectrochemical characterization of newly synthesized manganese, cobalt, iron and copper phthalocyanines, Electrochim. Acta 87 (2013) 554-566.

[70] D. Quinton, E. Antunes, S. Griveau, T. Nyokong, F. Bedioui, Cyclic voltammetry and spectroelectrochemistry of a novel manganese phthalocyanine substituted with hexynyl groups, Inorg. Chem. Commun. 14 (2011) 330-332.

[71] O.A. Osmanbas, A. Koca, I. Ozcesmeci, A.I. Okur, A. Gul, Voltammetric, spectroelectrochemical, and electrocatalytic properties of thiol-derivatized phthalocyanines, Electrochim. Acta 53 (2008) 4969-4680.

[72] C. Apetrei, S. Casilli, M. De Luca, L. Valli, J. Jiang, M.L. Rodriguez-Mendez, J.A. De Saja, Spectroelectrochemical characterisation of Langmuir–Schaefer films of heteroleptic phthalocyanine complexes. Potential applications, Colloid Surface A 284 (2006) 574-582.

[73] P.E. Smolenyak, E.J. Osburn, S.Y. Chen, L.K. Chau, D.F. OBrien, N.R. Armstrong, LB films of unusual octasubstituted phthalocyanines: Spectroelectrochemical and scanning probe microscopic characterization, Abstr. Pap. Am. Chem. S. 213 (1997) 143-COLL.

[74] D. Masheder, K.P.J. Williams, Raman spectro-electrochemistry. II. *In situ* raman spectroscopic studies of the electrochemical reduction of CO_2 at cobalt(II) phthalocyanine-impregnated PTFE-bonded carbon gas diffusion electrodes , J. Raman Spectrosc. 18 (1987) 391-398.

Figures and Scheme Captions

Fig. 1 Absorption spectra of novel synthesized compounds (**a** for **H_2Pc**, **b** for **ZnPc**, **c** for **PbPc**, **d** for **CoPc**, **e** for **CuPc**).

Fig. 2 (**a**) CVs of **H_2Pc** at various scan rates on a Pt working electrode in DCM/TBAP and (**b**) SWV of **H_2Pc** recorded with SWV parameters: step size = 5 mV; pulse size = 100 mV; Frequency = 25 Hz.

Fig. 3 (**a**) CVs of **ZnPc** at various scan rates on a Pt working electrode in DCM/TBAP and (**b**) SWV of **ZnPc** recorded with SWV parameters: step size = 5 mV; pulse size = 100 mV; Frequency = 25 Hz.

Fig. 4 (**a**) CVs of **PbPc** at various scan rates on a Pt working electrode in DCM/TBAP and (**b**) SWV of **PbPc** recorded with SWV parameters: step size = 5 mV; pulse size = 100 mV; Frequency = 25 Hz.

Fig. 5 CV and SWV of **CoPc** recorded at 0.100 Vs^{-1} scan rate on a Pt working electrode in DCM/TBAP.

Fig. 6 *In-situ* UV-Vis spectral changes of **H_2Pc** in DCM/TBAP. **a**) E_{app}= -0.85 V. **b**) E_{app}= -1.30 V. **c**) E_{app}= = 1.00 V.

Fig. 7 Fig. 7. *In-situ* UV-Vis spectral changes of **PbPc** recorded during reduction reactions in DCM/TBAP. **a**) Former part of the spectral changes at E_{app}= -0.75 V **b**) latter part of the spectral changes at E_{app}= -0.75 V). **c**). E_{app}= -1.30 V. **d**) Chromaticity diagram (each symbol represents the color of electro-generated species; □: $[Pb^{II}Pc^{-2}]$, ○:$[H_2Pc^{-2}]$ △: $[H_2Pc^{-3}]^{-2}$;☆: $[Pb^{II}Pc^{-1}]^{+1}$.

Fig. 8. *In-situ* UV-Vis spectral changes of **PbPc** recorded during oxidation reactions in DCM/TBAP. **a**) E_{app}= 1.00 V. **b**) E_{app}= 1.50 V.

Fig. 9 *In-situ* UV-Vis spectral changes of **CoPc** in DCM/TBAP. **a**) E_{app}= -0.75 V. **b**) E_{app}= = 1.00 V. **c**) Chromaticity diagram (each symbol represents the color of electro-generated species; □: $[Co^{II}Pc^{-2}]$, ○:$[Co^{I}Pc^{-2}]^{-1}$☆: $[Co^{II}Pc^{-1}]^{+1}$.

Scheme 1. Synthesis of dinitrile compound (**3**) and novel phthalocyanines (**4-8**). Reaction conditions: *i*: anhydrous K_2CO_3, dry DMF, 50 ^{0}C; *ii*: *n*-pentanol, 1,8-diazabicyclo[5.4.0]undec-7-ene and related metal salts ($Zn(CH_3COO)_2$, PbO, $CoCl_2$, $CuCl_2$) at 160 ^{o}C.

Table 1. Absorption spectral data for the substituted **H_2Pc** (**4**), **ZnPc** (**5**), **CoPc** (**6**), **PbPc** (**7**) and **CuPc** (**8**) compounds in THF.

Compound	$\lambda_{max,}$ nm (logε)	
	B band	Q band
H_2Pc (4)	383 (4.78)	605 (4.68), 638 (4.81), 665 (5.16), 700 (5.20)
ZnPc (5)	328 (5.02), 356 (4.96)	607 (4.63), 673 (5.30)
CoPc (6)	313 (5.21), 354 (4.91)	601 (4.64), 667 (5.26)
PbPc (7)	363 (4.87)	638 (4.60), 707 (5.29)
CuPc (8)	348 (4.94)	608 (4.75), 675 (5.29)

Table 2. Voltammetric data of the complexes. All voltammetric data were given versus SCE.

Complex		Ring Oxidations		M^{II}/M^{I}	Ring Reductions	
H_2Pc (4)	[a]$E_{1/2}$	1.12	0.92	-	-0.62	-0.91
	[b]ΔE_p (mV)	72	65	-	59	60
	[c]$I_{p,a}/I_{p,c}$	0.91	0.93	-	0.98	0.96
ZnPc (5)	[a]$E_{1/2}$	-	0.75	-	-1.01 (-0.87)[d]	-1.30
	[b]ΔE_p (mV)	-	85	-	96	130
	[c]$I_{p,a}/I_{p,c}$	-	0.78	-	1.47	0.75
PbPc (6)	[a]$E_{1/2}$	1.33	0.83	-	-0.61	-0.94
	[b]ΔE_p (mV)	85	110	-	80	90
	[c]$I_{p,a}/I_{p,c}$	0.55	0.83	-	0.95	0.90
CoPc (7)	[a]$E_{1/2}$	-	0.78	-0.05 (-0.55)[d]	-1.31	-
	[b]ΔE_p (mV)	-	110	168	120	-
	[c]$I_{p,a}/I_{p,c}$	-	0.95	0.86	0.81	-

[a]:$E_{1/2}$ values ((E_{pa}+E_{pc})/2) were given versus SCE at 0.100 Vs^{-1} scan rate. **[b]:** $\Delta E_p = E_{pa}-E_{pc}$. **[c]**: $I_{p,a}/I_{p,c}$ for reduction ,$I_{p,c}/I_{p,a}$for oxidation processes. **[d]**peak potential of the aggregated species were given in parentheses.

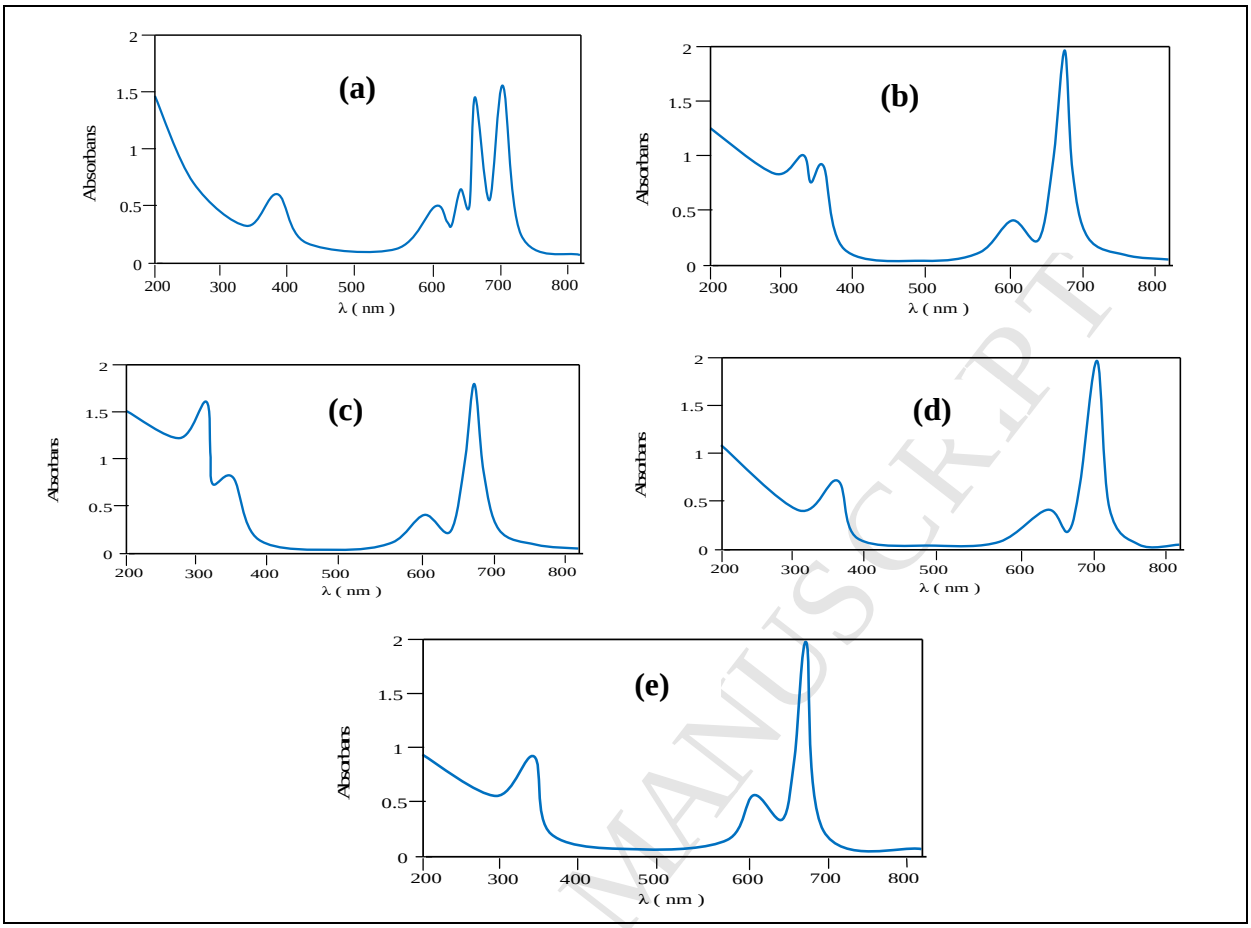

Fig. 1. Absorption spectra of novel synthesized compounds (**a** for **H_2Pc**, **b** for **ZnPc**, **c** for **PbPc**, **d** for **CoPc**, **e** for **CuPc**).

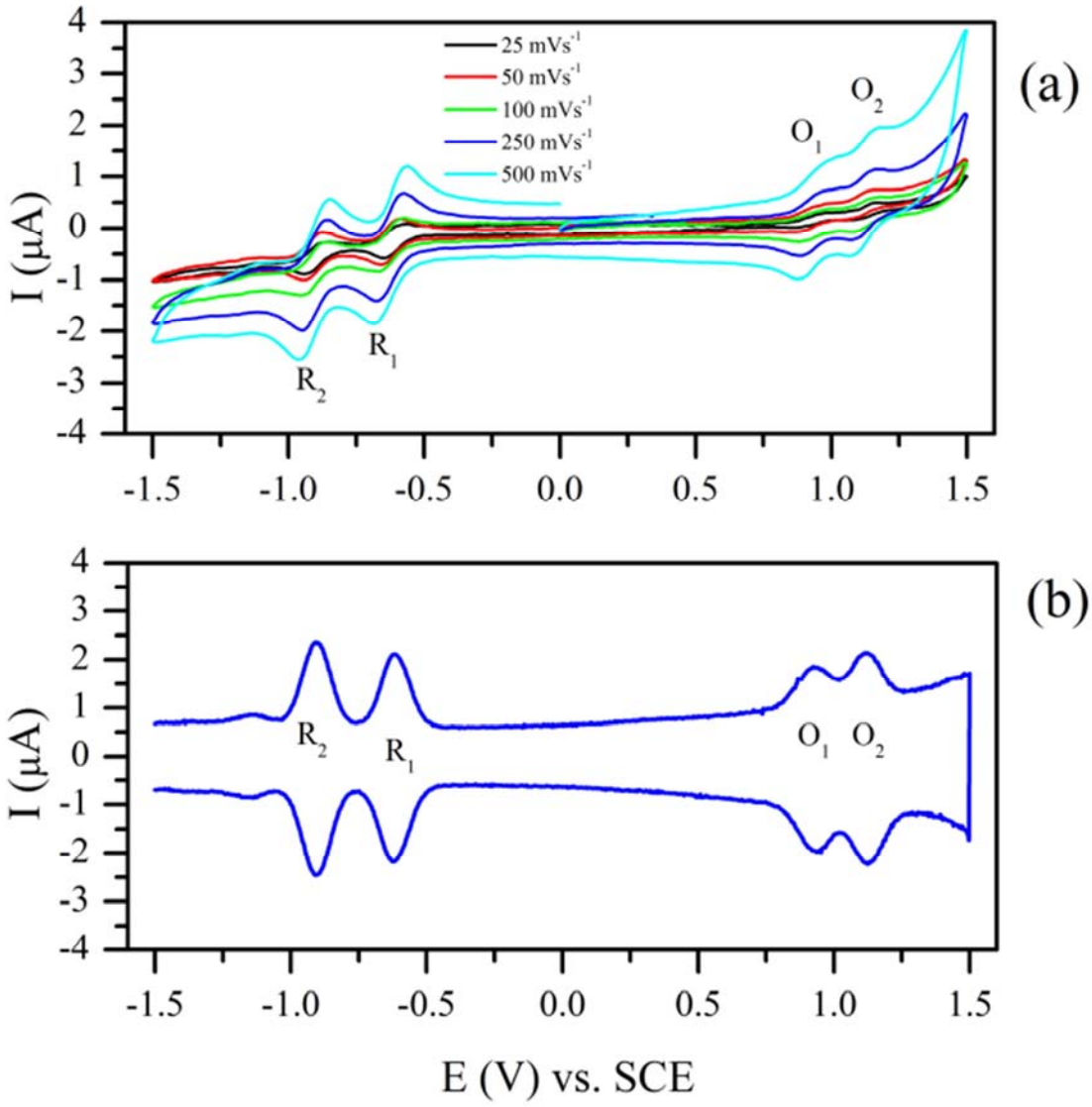

Fig. 2. (**a**) CVs of **H_2Pc** at various scan rates on a Pt working electrode in DCM/TBAP and (**b**) SWV of **H_2Pc** recorded with SWV parameters: step size = 5 mV; pulse size = 100 mV; Frequency = 25 Hz.

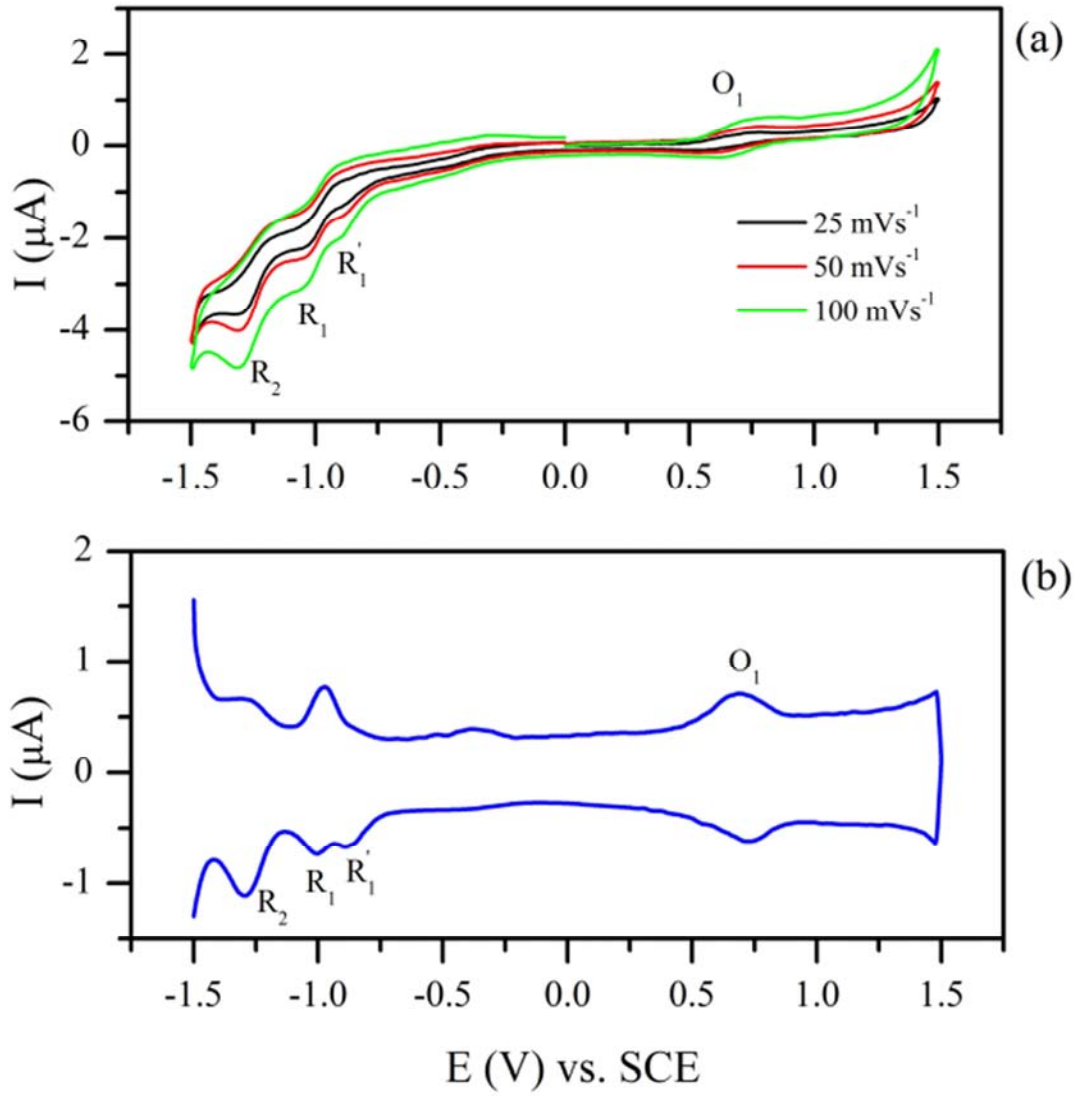

Fig.3. (**a**) CVs of **ZnPc** at various scan rates on a Pt working electrode in DCM/TBAP and (**b**) SWV of **ZnPc** recorded with SWV parameters: step size = 5 mV; pulse size = 100 mV; Frequency = 25 Hz.

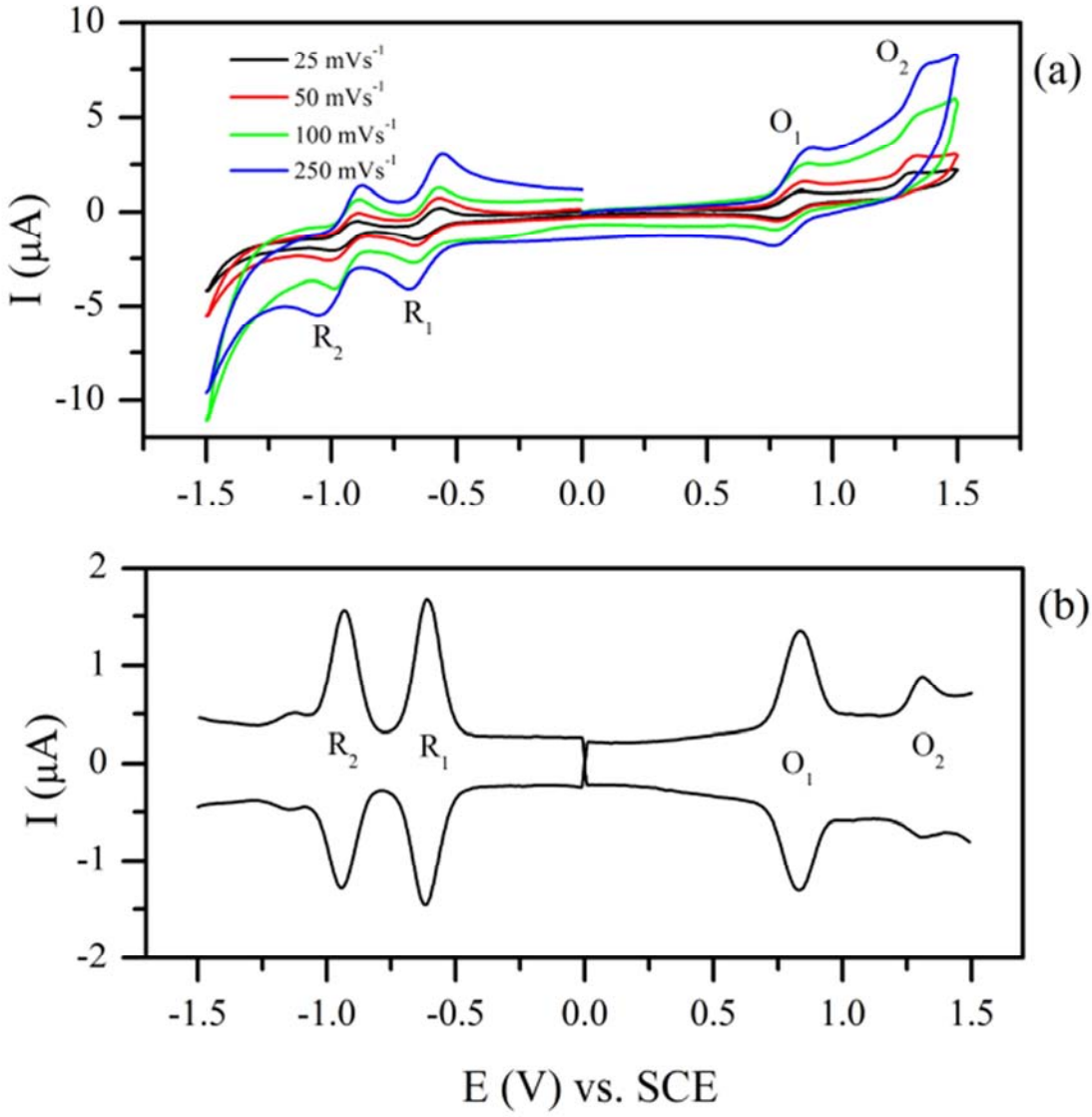

Fig. 4. (**a**) CVs of **PbPc** at various scan rates on a Pt working electrode in DCM/TBAP and (**b**) SWV of **PbPc** recorded with SWV parameters: step size = 5 mV; pulse size = 100 mV; Frequency = 25 Hz.

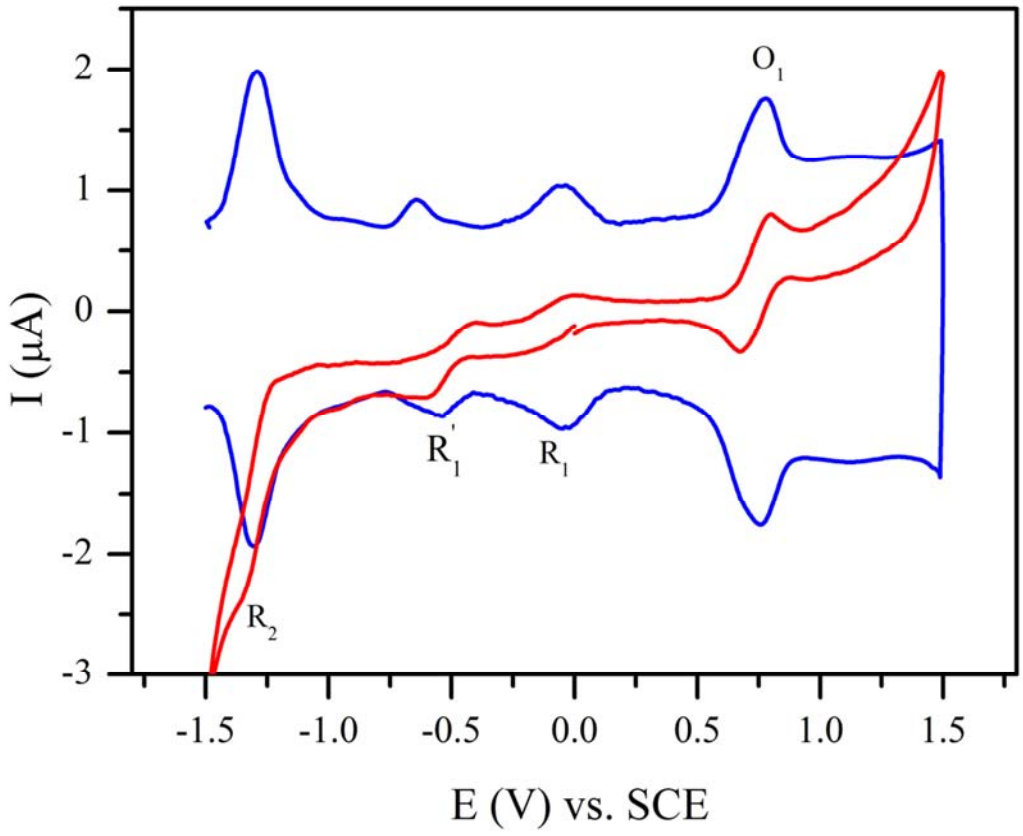

Fig. 5. CV and SWV of **CoPc** recorded at 0.100 Vs^{-1} scan rate on a Pt working electrode in DCM/TBAP .

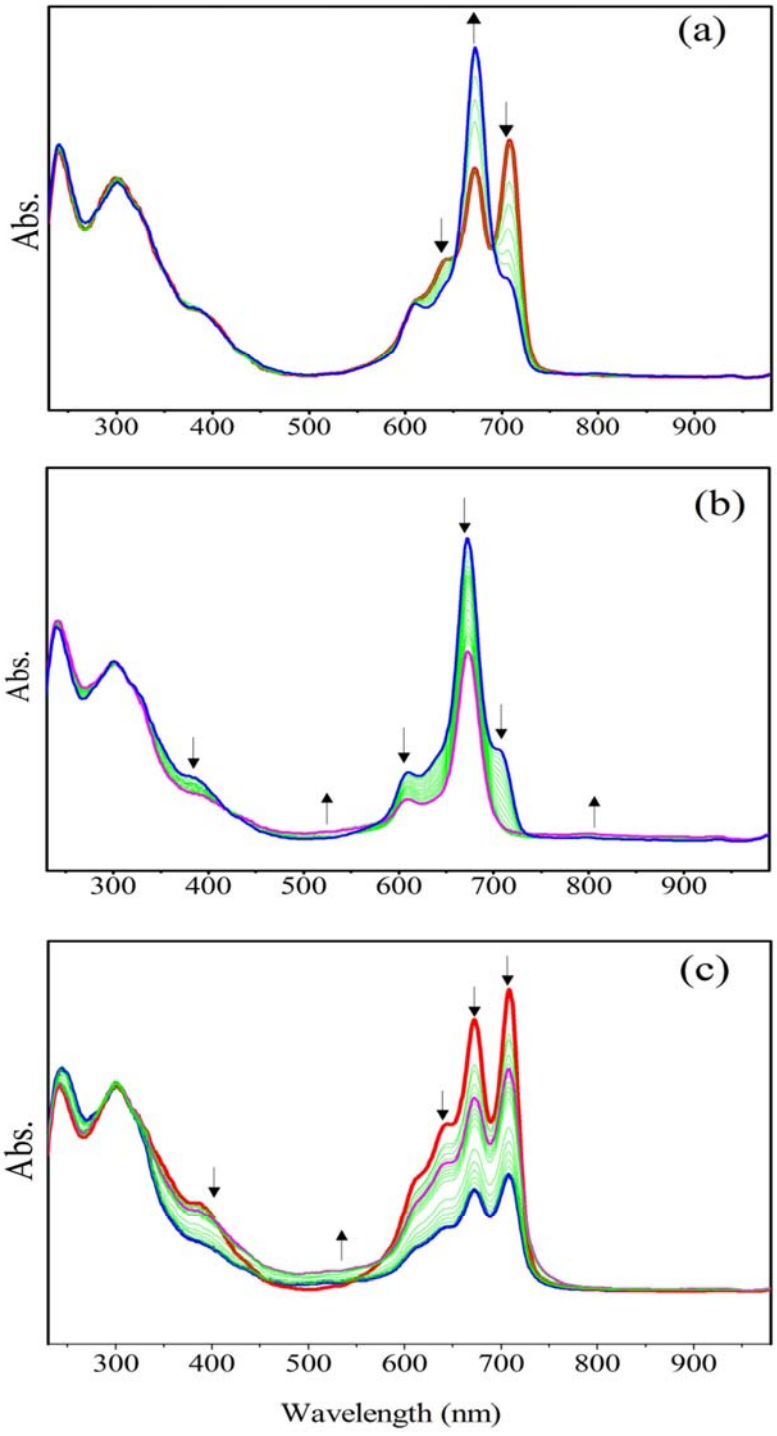

Fig. 6. *In-situ* UV-Vis spectral changes of **H_2Pc** in DCM/TBAP. **a**) E_{app}= -0.85 V. **b**) E_{app}= -1.30 V. **c**) E_{app}= = 1.00 V.

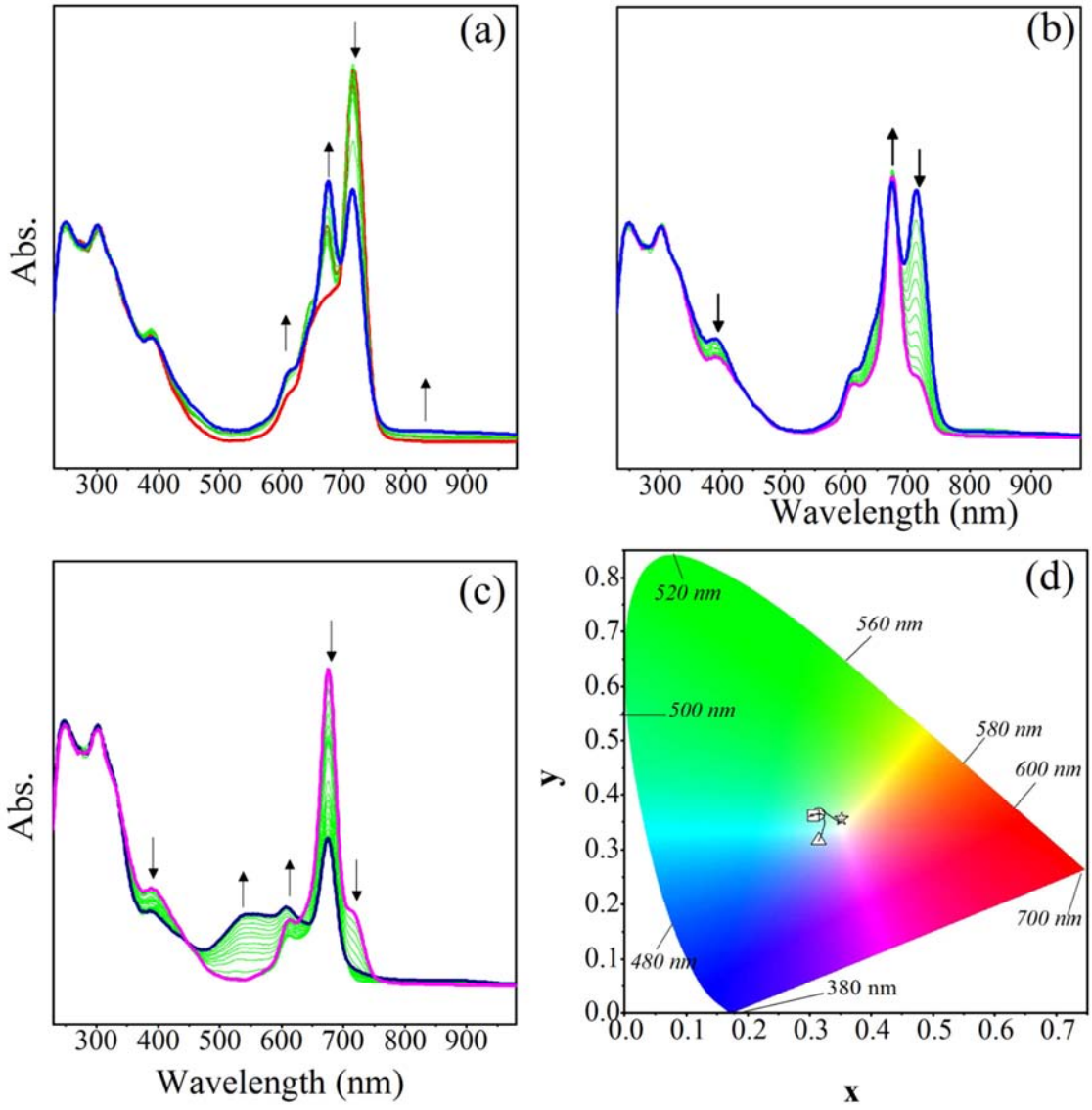

Fig. 7. *In-situ* UV-Vis spectral changes of **PbPc** recorded during reduction reactions in DCM/TBAP. **a**) Former part of the spectral changes at E_{app}= -0.75 V **b**) latter part of the spectral changes at E_{app}= -0.75 V). **c**). E_{app}= -1.30 V. **d**) Chromaticity diagram (each symbol represents the color of electro-generated species; □: $[Pb^{II}Pc^{-2}]$, ○:$[H_2Pc^{-2}]$ △: $[H_2Pc^{-3}]^{-2}$;☆: $[Pb^{II}Pc^{-1}]^{+1}$.

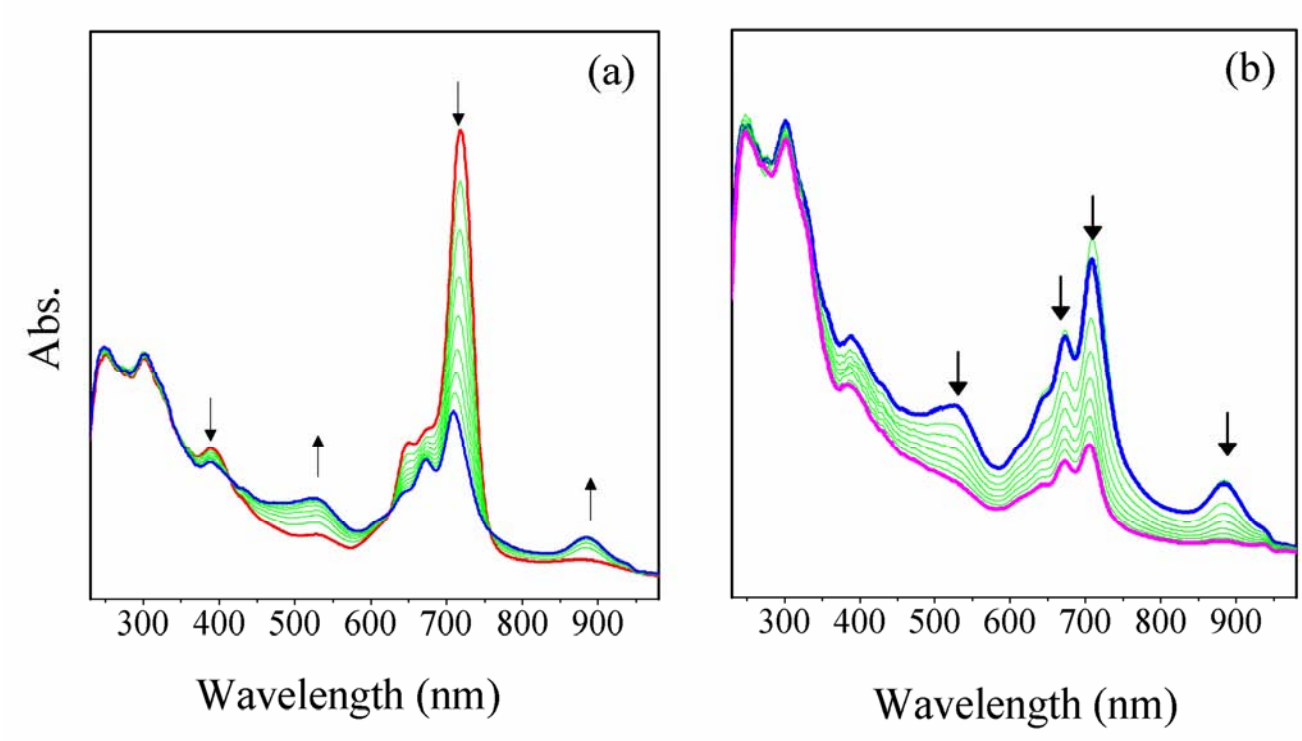

Fig. 8. *In-situ* UV-Vis spectral changes of **PbPc** recorded during oxidation reactions in DCM/TBAP. **a**) E_{app}= 1.00 V. **b**) E_{app}= 1.50 V.

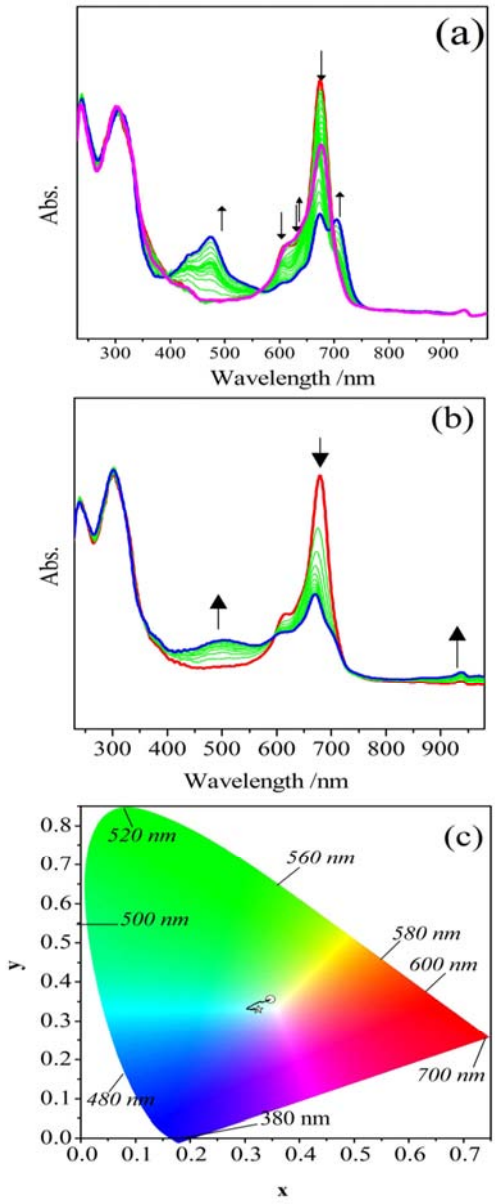

Fig. 9. *In-situ* UV-Vis spectral changes of **CoPc** in DCM/TBAP. **a**) E_{app}= -0.75 V. **b**) E_{app}= = 1.00 V. **c**) Chromaticity diagram (each symbol represents the color of electro-generated species; □: $[Co^{II}Pc^{-2}]$, ○:$[Co^{I}Pc^{-2}]^{-1}$ ☆ : $[Co^{II}Pc^{-1}]^{+1}$.

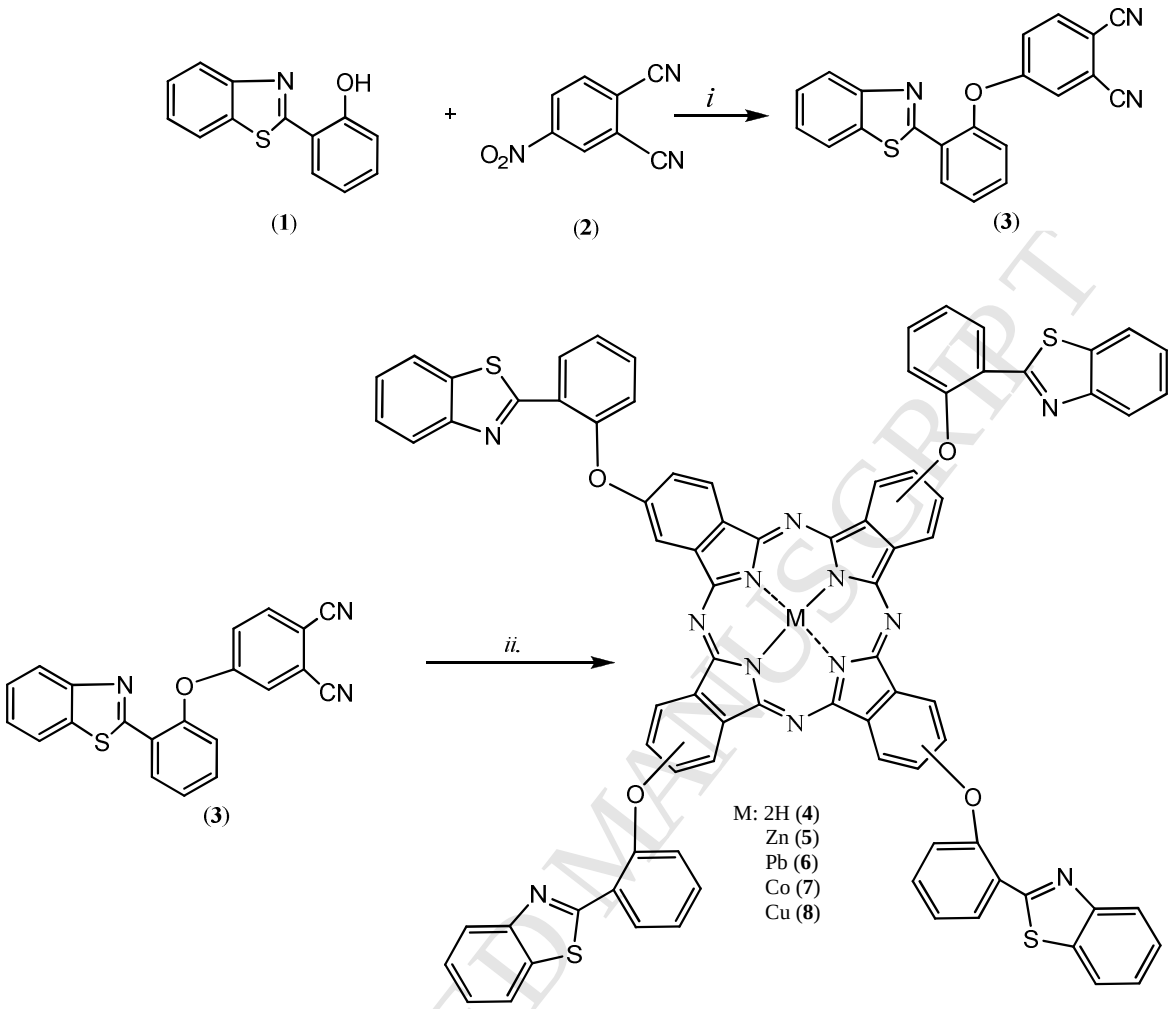

Scheme 1. Synthesis of dinitrile compound (**3**) and novel phthalocyanines (**4-8**). Reaction conditions: *i*: anhydrous K_2CO_3, dry DMF, 50 ^{0}C; *ii*: *n*-pentanol, 1,8-diazabicyclo[5.4.0]undec-7-ene and related metal salts ($Zn(CH_3COO)_2$, PbO, $CoCl_2$, $CuCl_2$) at 160 ^{o}C.

HIGHLIGHTS

Novel 4-(2-(benzo[d]thiazol-2-yl)phenoxy) substituted phthalocyanine derivatives: Synthesis, electrochemical and *in situ* spectroelectrochemical characterization

Asiye Nas[a], Halit Kantekin[a], Atıf Koca[b]

- The synthesis and characterization of novel *4-(2-(benzo[d]thiazol-2-yl)phenoxy*-substituted metal-free (**4**), zinc(II) (**5**), lead(II) (**6**), cobalt(II) (**7**) and copper(II) (**8**) phthalocyanine derivatives
- Voltammetric characterizations of the complexes (**4-7**) with cyclic voltammetry and square wave voltammetry
-Reversible reduction and oxidation reactions of **PbPc** (**6**) during the CV and SWV measurements

SUPPLEMENTARY INFORMATION

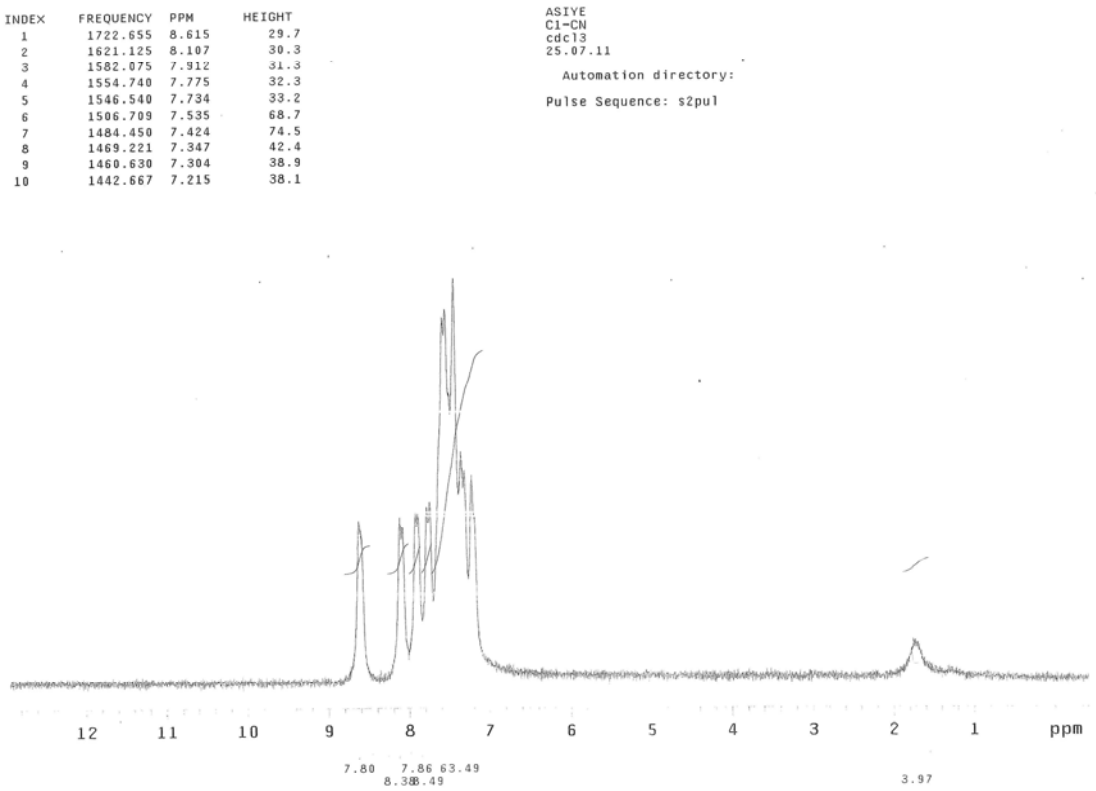

INDEX	FREQUENCY	PPM	HEIGHT
1	1722.655	8.615	29.7
2	1621.125	8.107	30.3
3	1582.075	7.912	31.3
4	1554.740	7.775	32.3
5	1546.540	7.734	33.2
6	1506.709	7.535	68.7
7	1484.450	7.424	74.5
8	1469.221	7.347	42.4
9	1460.630	7.304	38.9
10	1442.667	7.215	38.1

Fig. S1. ^{1}H NMR spectrum of compound **3** in $CDCl_3$.

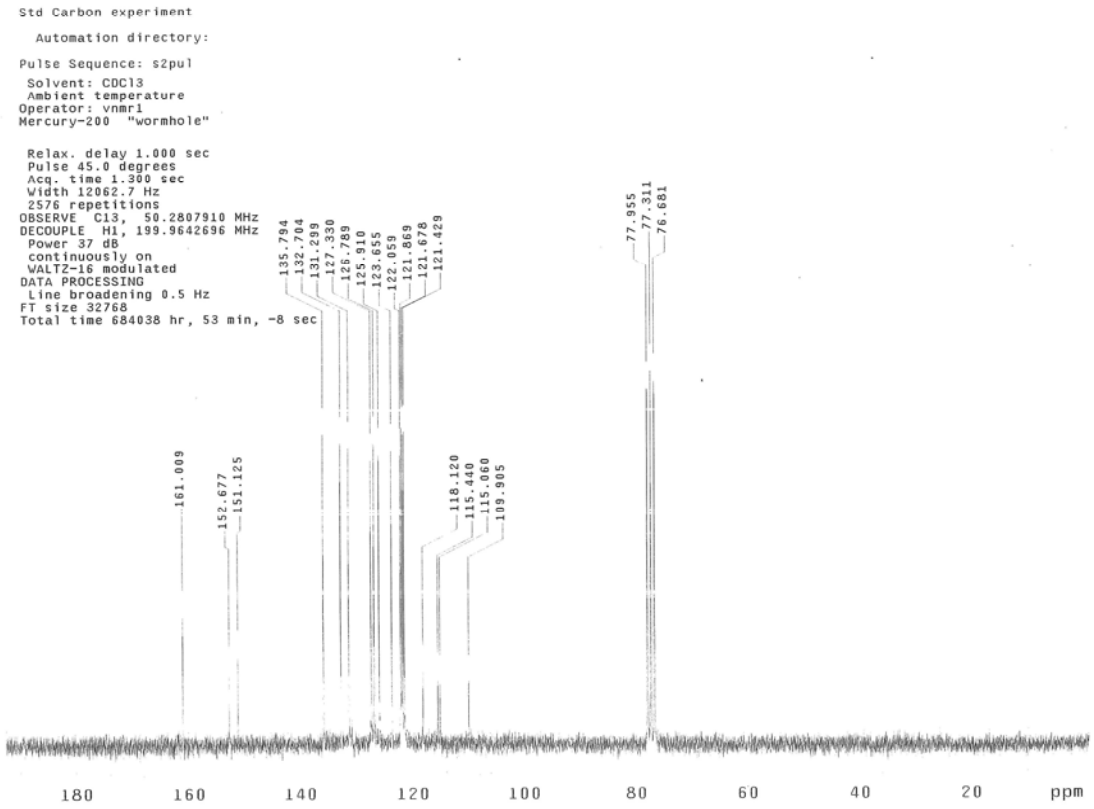

Fig. S2. ^{13}C NMR spectrum of compound **3** in $CDCl_3$.

AC-NITRIL_DHB

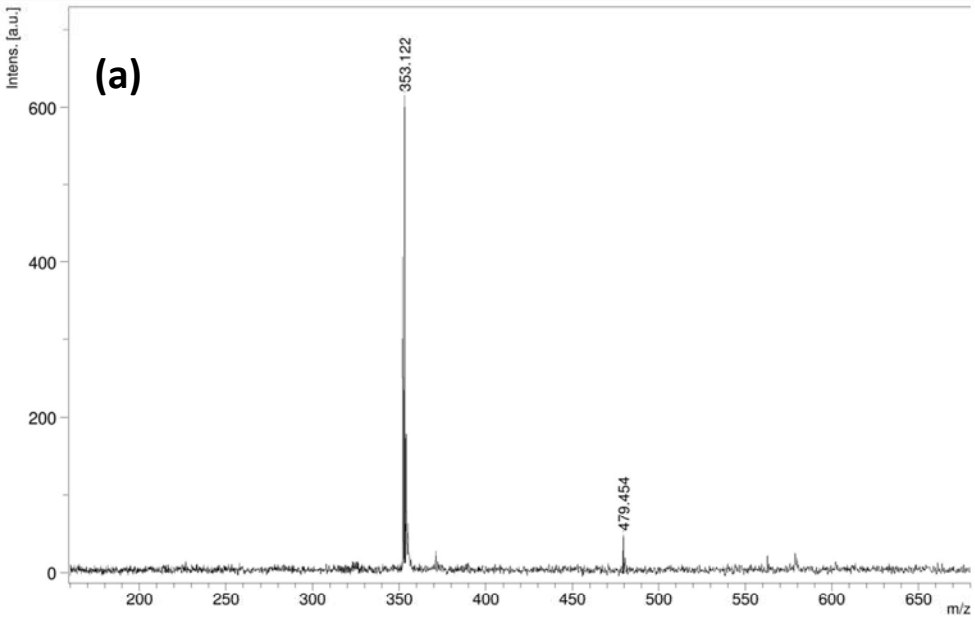

m/z	SN	Quality Fac.	Res.	Intens.	Area
353.122	76.4		996	613.97	254
479.454	5.9		1177	47.55	21

Date of Acquisition 2013-03-27T14:00:23.000

File Name D:\Data\bcosut\AC-NITRIL_DHB\0_G1\1

Performed by Date / Sign

Viewed by Date / Sign

BRUKER DALTONICS

printed:3/27/2013 2:00:42 PM

AC-METAL-FREE_DHB

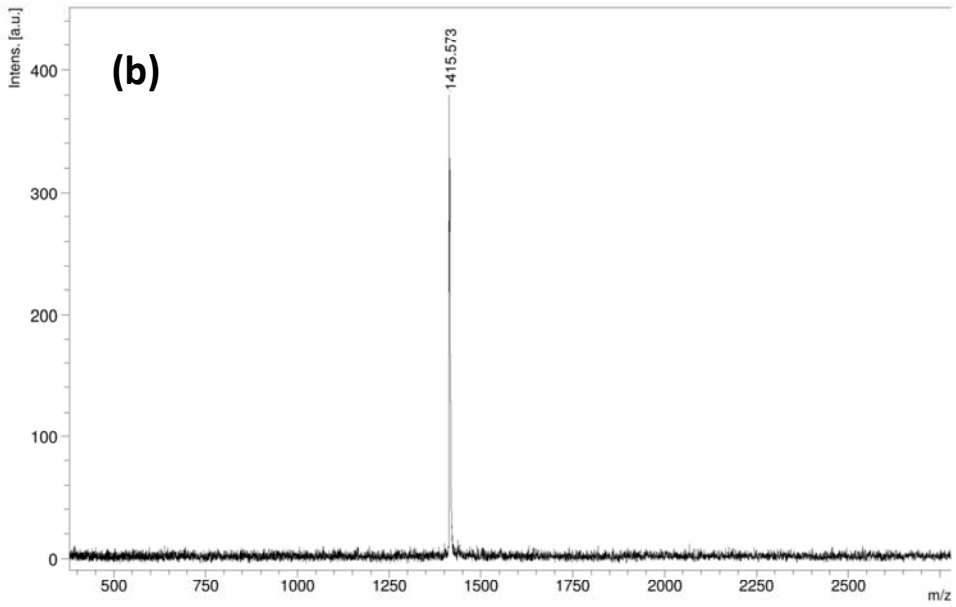

m/z	SN	Quality Fac.	Res.	Intens.	Area
1415.573				318.83	

Date of Acquisition 2013-03-22T08:13:44.000

File Name D:\Data\bcosut\AC-METAL-FREE_DHB\0_F12\1

Performed by Date / Sign

Viewed by Date / Sign

printed:3/22/2013 8:14:07 AM

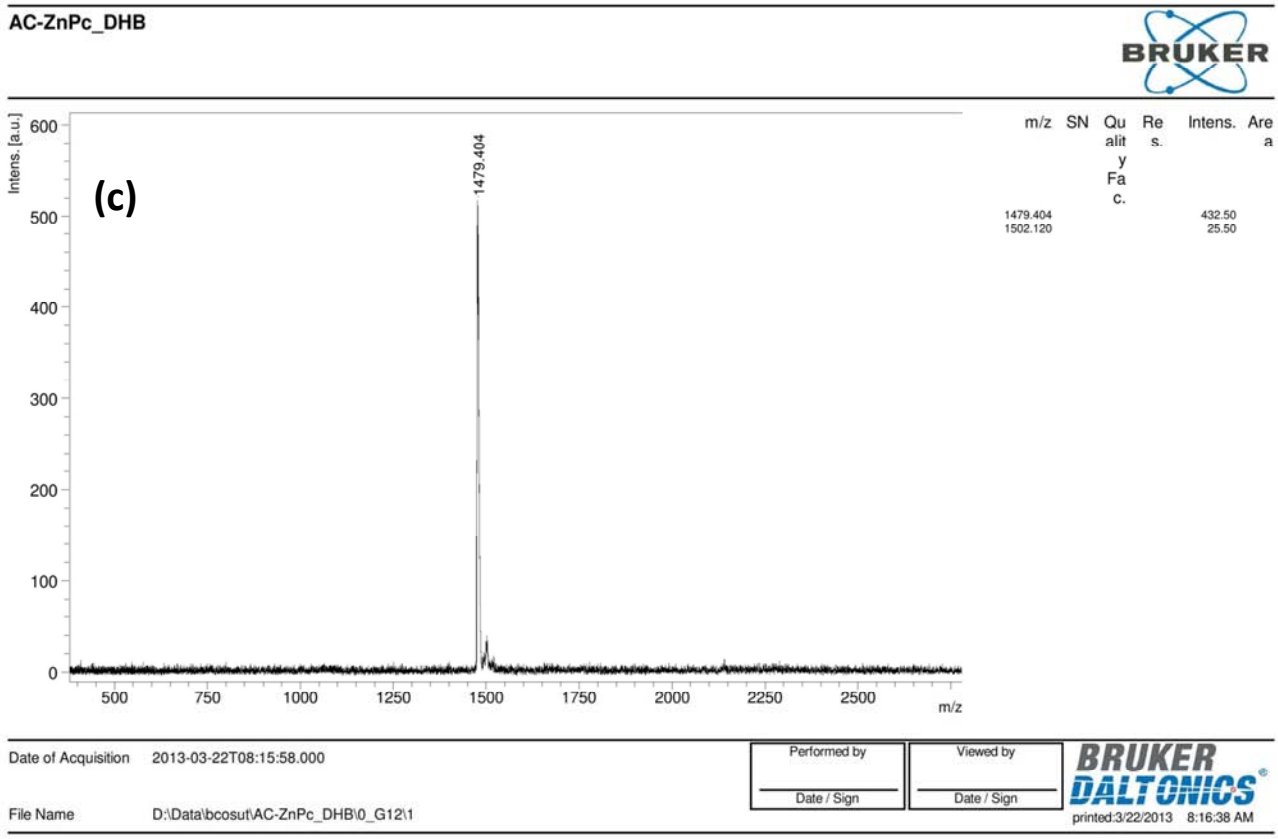

Fig. S3. MALDI-MS spectra of novel synthesized compounds (**a** for compound **3**, **b** for **H_2Pc**, **c** for **ZnPc**).

AC-PbPc_NO M

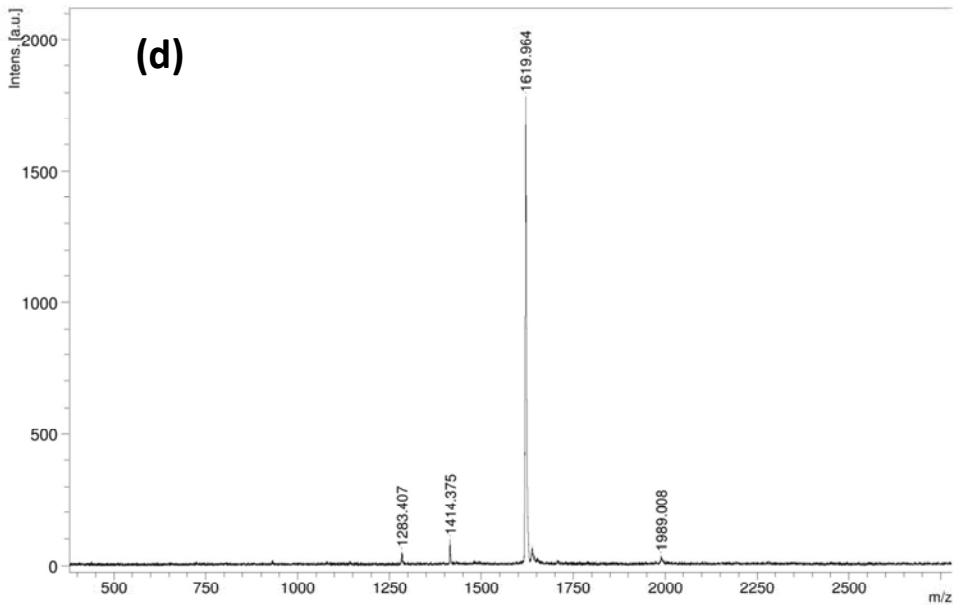

m/z	SN	Quality Fac.	Res.	Intens.	Area
1283.407	5.4		2711	45.00	28
1414.375	8.0		2673	69.00	50
1619.964	176.5		2809	1634.00	1522
1989.008	2.6		2585	23.00	23

Date of Acquisition 2013-03-22T09:03:50.000

File Name D:\Data\bcosut\AC-PbPc_NO M\0_H6\1

Performed by
Date / Sign

Viewed by
Date / Sign

BRUKER DALTONICS
printed:3/22/2013 9:04:12 AM

AC-COPC_DHB

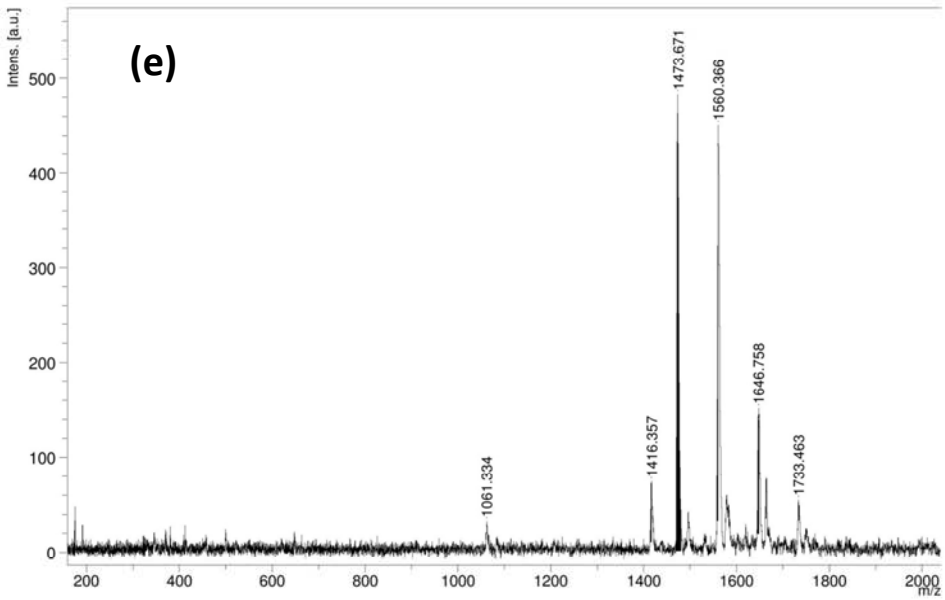

m/z	SN	Quality Fac.	Res.	Intens.	Area
1061.334	2.6		3901	26.00	11
1416.357	6.4		1190	72.78	101
1473.671	41.2		330	482.65	2355
1560.366	36.1		868	449.68	866
1577.132	4.6		2592	58.51	60
1646.758	10.8		1139	143.76	251
1663.313	5.8		2207	77.35	105
1733.463	4.1		999	54.06	116

Date of Acquisition 2013-03-27T14:03:10.000

File Name D:\Data\bcosut\AC-COPC_DHB\0_G5\1

Performed by Date / Sign

Viewed by Date / Sign

printed:3/27/2013 2:04:12 PM

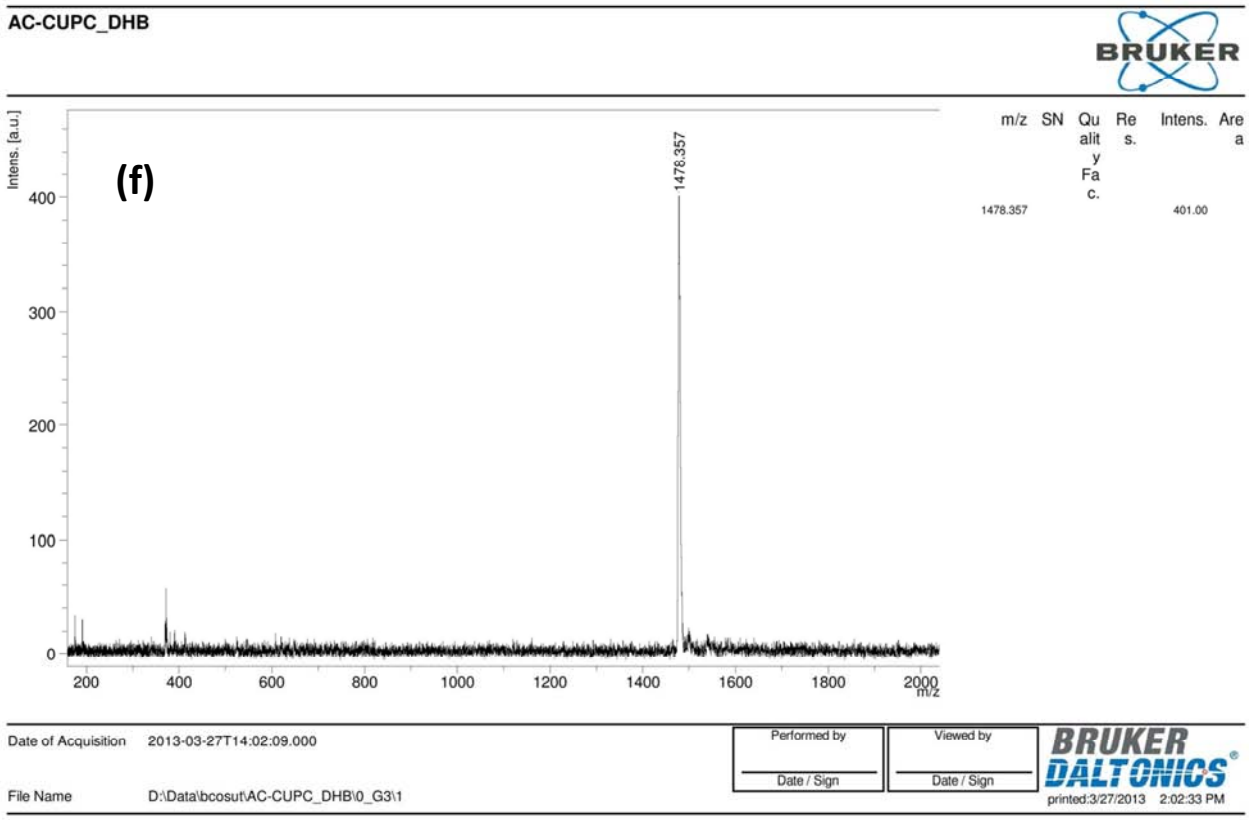

Fig. S4. MALDI-MS spectra of novel synthesized compounds (**d** for **PbPc**, **e** for **CoPc, f** for **CuPc**).